
Semiconductor Devices

THIRD EDITION

S. M. Sze and M. K. Lee

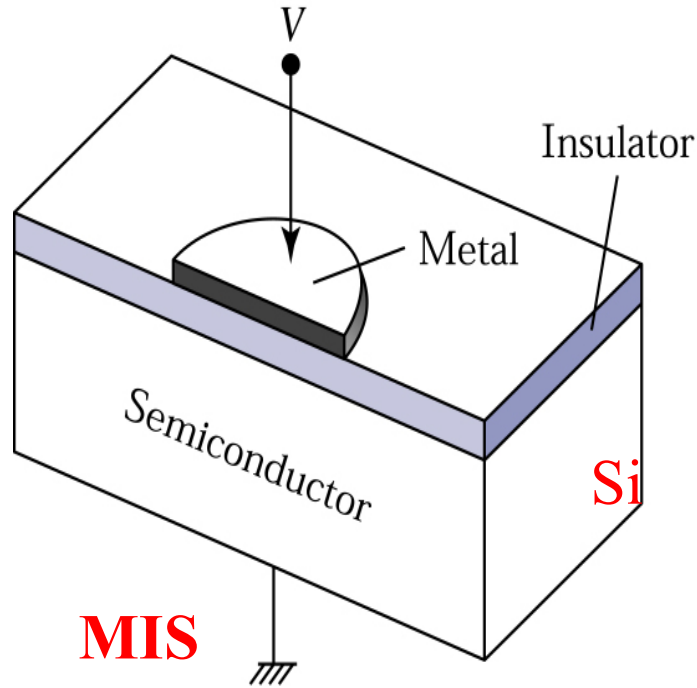
Chapter 5

MOS Capacitor and MOSFET

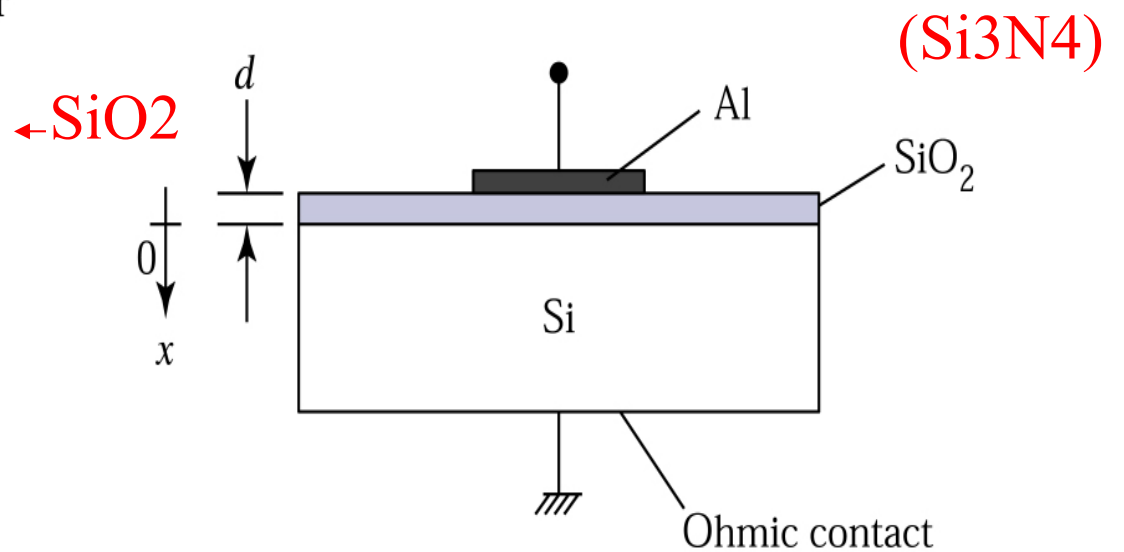
先令其

affinity

$$q\Phi_{ms} \equiv (q\Phi_m - q\Phi_s) = q\Phi_m - [q\chi + E_g / 2 + q\Psi_B] = 0 \quad (1)$$



(a)



(b)

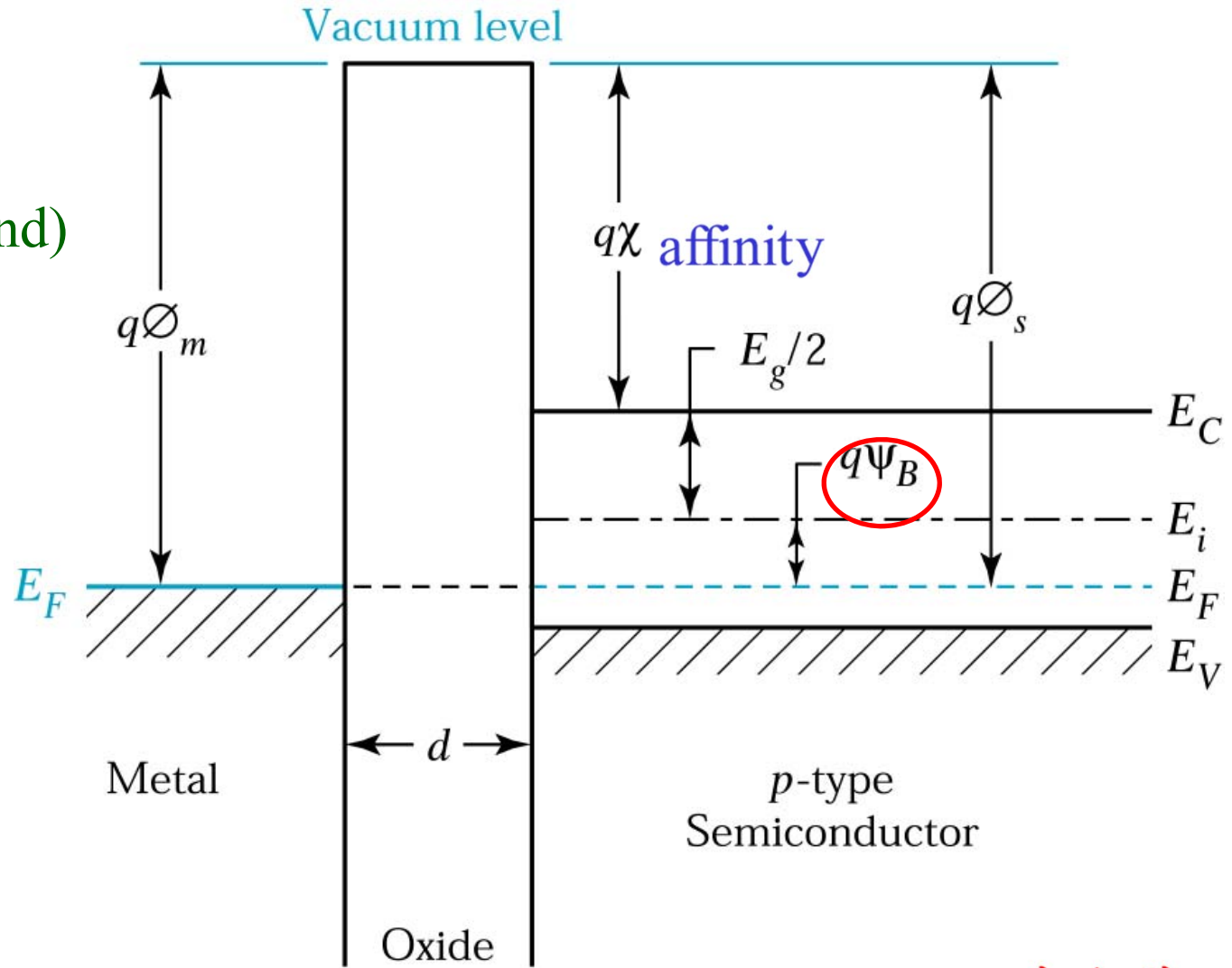
Figure 5.1. (a) Perspective view of a metal-oxide-semiconductor (MOS) diode. (b) Cross-section of an MOS diode.

Ideal MOS :

1. $\Phi_m = \Phi_s$ (flat band)

2. $Q_m = Q_s$, 某VG下

3. $R_{ox} \rightarrow \infty$



先令其

$$q\Phi_{ms} \equiv (q\Phi_m - q\Phi_s) = q\Phi_m - [q\chi + E_g / 2 + q\Psi_B] = 0$$

Figure 5.2. Energy band diagram of an ideal MOS diode at $V = 0$.

$$p_p = n_i e^{(E_i - E_F) / KT} \quad (2)$$

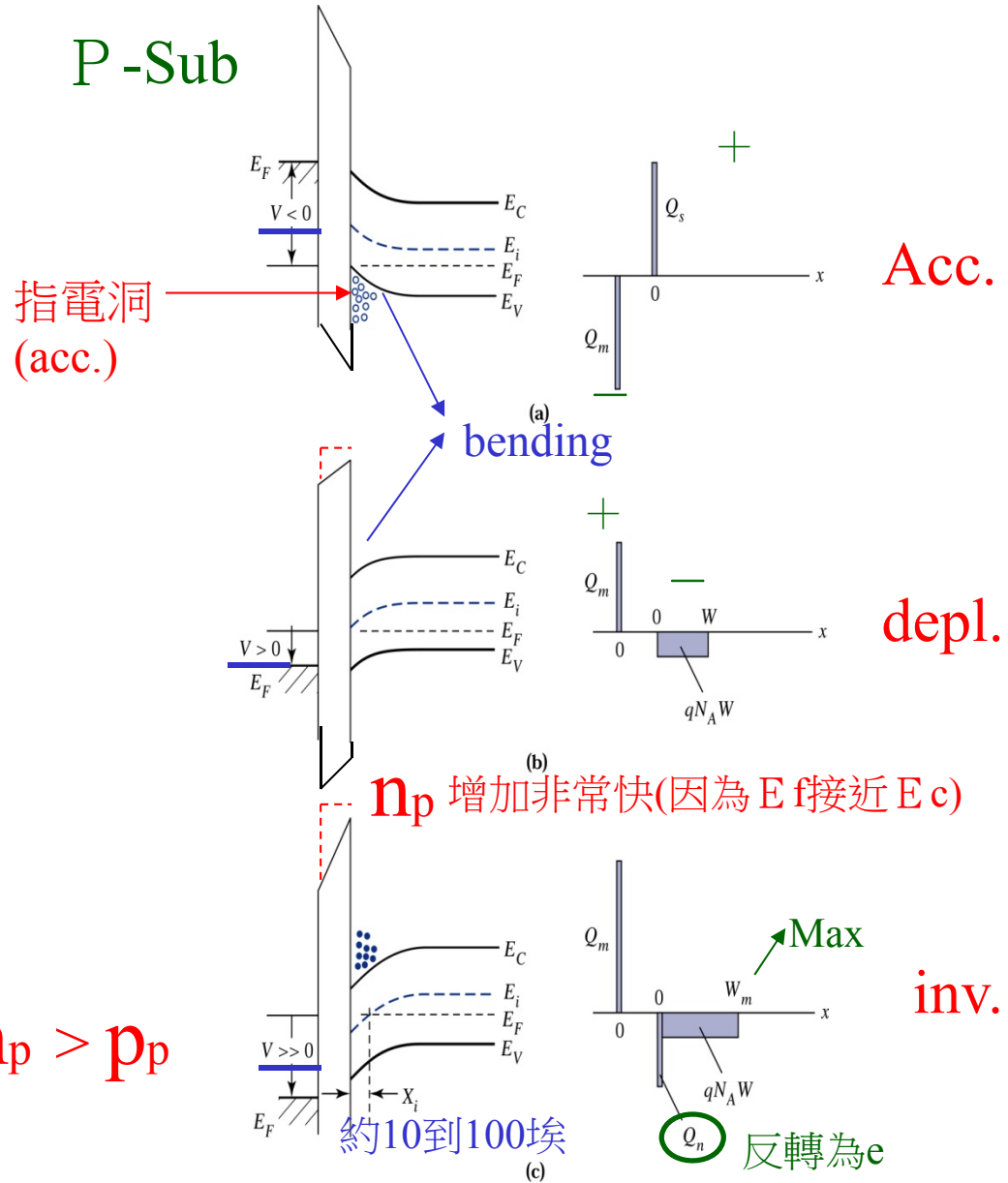
$$n_p = n_i e^{(E_F - E_i) / KT} \quad (3)$$

$E_F - E_i > 0, n_p \uparrow \uparrow$

$$Q_s = Q_n - Q_{sc} = -qN_A W \quad (3)$$

單位面積空間

Figure 5.3.
Energy band diagrams and charge distributions of an ideal MOS diode in (a) **accumulation**, (b) **depletion**, and (c) **inversion** cases.



$$Q_s = \overset{\text{Inv.}}{Q_n} + Q_{sc}$$

Strong inv. $Q_{sc} = -qN_A W_m$

固定 Max.

Strong inv. 後, 負 Q 大部分由 Q_n 提供

$$n_p > p_p$$

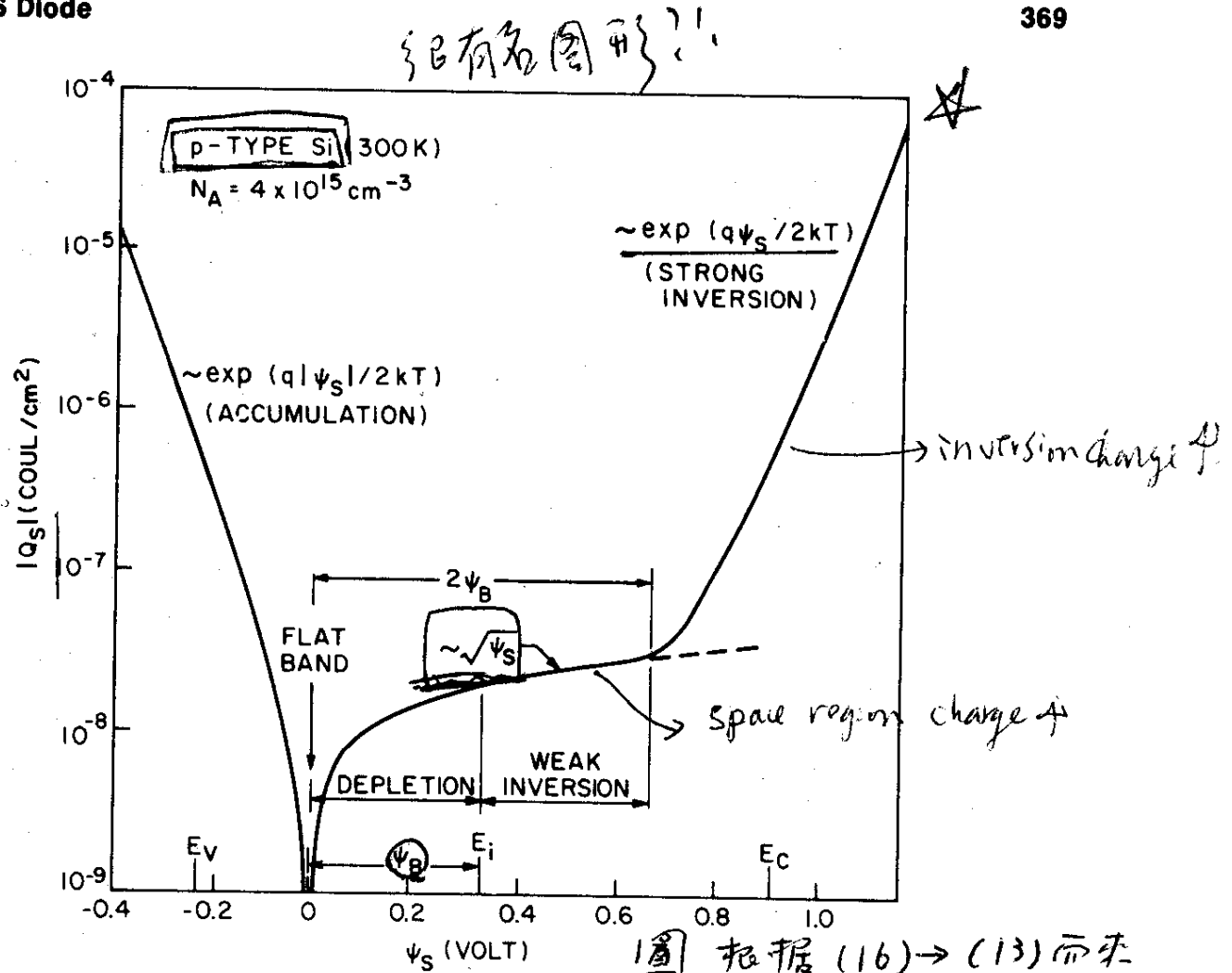


Fig. 5 Variation of space-charge density in the semiconductor as a function of the surface potential ψ_s for a p-type silicon with $N_A = 4 \times 10^{15} \text{ cm}^{-3}$ at room temperature; ψ_B the potential difference between the Fermi level and the intrinsic level of the bulk semiconductor. (After Garrett and Brattain, Ref. 13.)

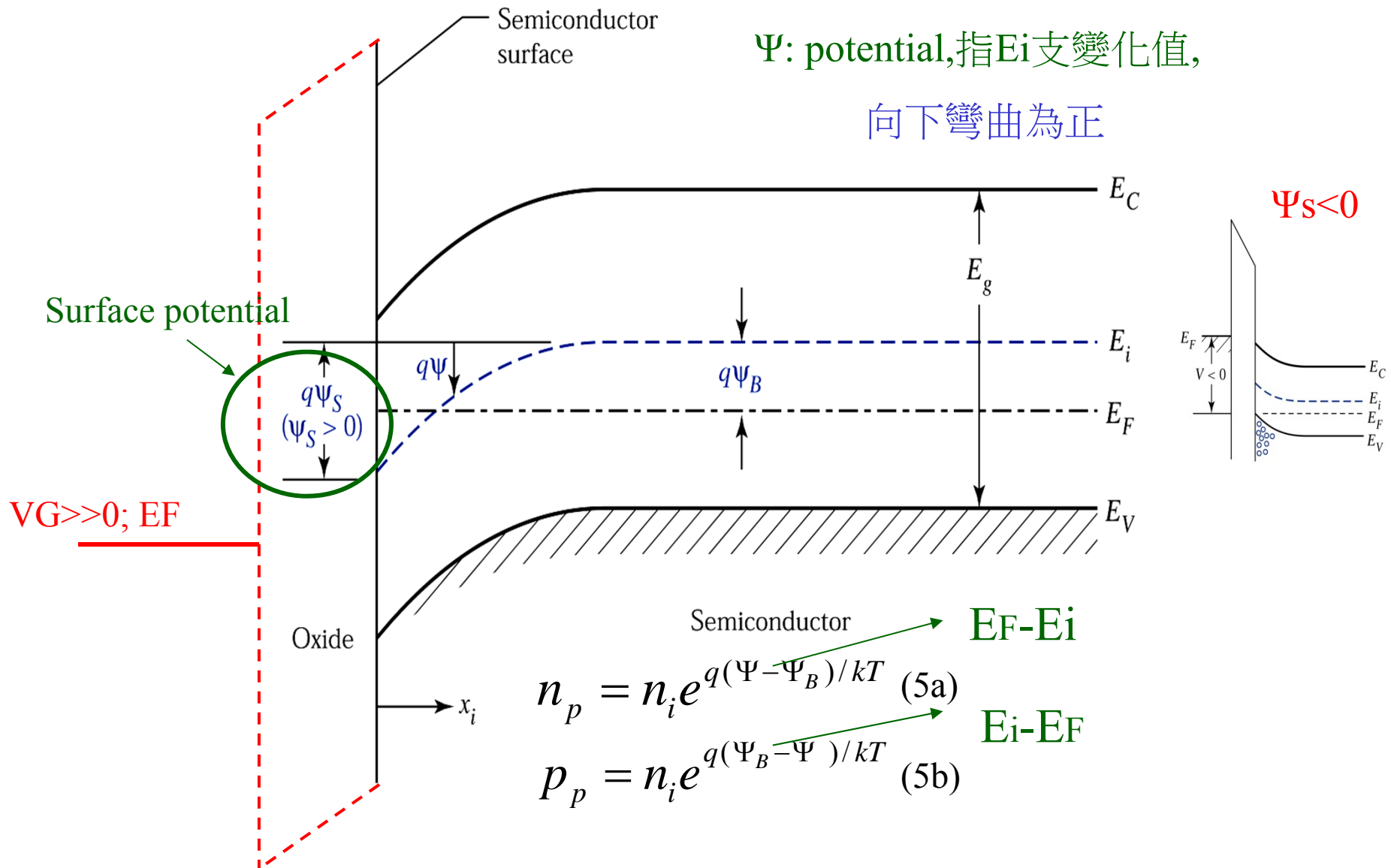


Figure 5.4. Energy band diagrams at the surface of a p -type semiconductor.

$\psi_s < 0$	Accumulation of holes (<u>bands bend upward</u>)
$\psi_s = 0$	<u>Flat-band</u> condition 在Si為平的
$\psi_B > \psi_s > 0$	Depletion of holes (bands bend downward)
$\psi_s = \psi_B$	<u>Midgap</u> with $n_s = n_p = n_i$ (intrinsic concentration)
$\psi_s > \psi_B$	Inversion (bands bend downward as shown in Fig. 24).
$\psi_s = 2\psi_B$	Strong inv. ($n_s = N_A$) $E_F - E_i = \Psi_B$

Poisson equation :

$$\frac{d^2\Psi}{dx^2} = \frac{-\rho_s(x)}{\epsilon_s} \quad (7)$$

$$\frac{d\Psi}{dx} = \int_W^x \frac{qN_A}{\epsilon_s} dx = (x - W) \frac{qN_A}{\epsilon_s}$$

$$\Psi = \Psi_s \left[1 - \frac{x}{W}\right]^2$$

(8)

$$\begin{aligned} \Psi &= \frac{qN_A}{\epsilon_s} \left(\frac{x^2}{2} - Wx\right) \Big|_W^x \\ &= \frac{qN_A}{2\epsilon_s} W^2 \left(1 - \frac{x}{W}\right)^2 \end{aligned}$$

Surface potential Ψ_s is ($x=0$ 之 Ψ) 像n+p junction

$$\Psi_s = \frac{qN_A W^2}{2\epsilon_s} \quad (9)$$

定義 strong inv. : (W 達 W_{max})

$$\begin{aligned} n_s = N_A & \longleftrightarrow \psi_s = 2\psi_B \\ \text{即 } \Psi_s(inv) & \approx 2\Psi_B = \frac{2KT}{q} \ln\left[\frac{N_A}{n_i}\right] \quad (10) \end{aligned}$$

Barrier ($V_{bi}-V$)

$$\text{Strong inv.} \left\{ W_m = \sqrt{\frac{2\epsilon_s \Psi_s(inv)}{qN_A}} \cong \sqrt{\frac{2\epsilon_s (2\Psi_B)}{qN_A}} = \sqrt{\frac{4\epsilon_s KT \ln(N_A/n_i)}{q^2 N_A}} \quad (11\&11a)$$

$$Q_{sc} = -qN_A W_m \cong -\sqrt{2q\epsilon_s N_A (2\Psi_B)} \quad (12)$$

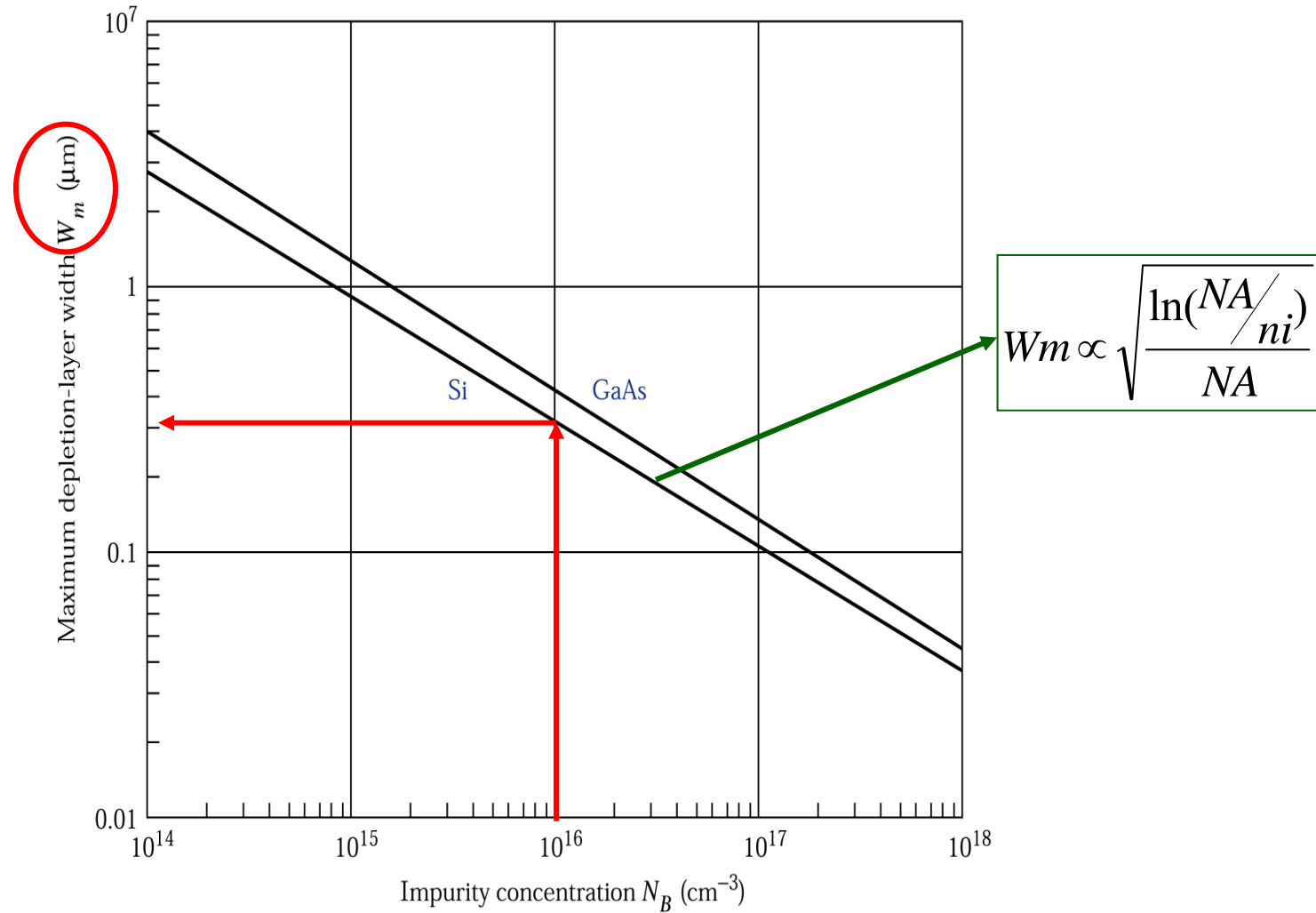


Figure 5.5. Maximum depletion-layer width versus impurity concentration of Si and GaAs under **strong-inversion** condition.

Ideal MOS curves (參看 F.6)

外加 \rightarrow $V = V_o + \Psi_s$ (13)

\swarrow SiO₂上

\searrow Si上

\swarrow Si單位面積電荷

$$V_o = E_o d = \frac{|Q_s| d}{\epsilon_{ox}} \equiv \frac{|Q_s|}{C_o} \quad (14)$$

\rightarrow 單位面積電容

(C=C_o串C_j) $C = \frac{C_o C_j}{C_o + C_j}$ (15)

\swarrow 空乏區電容

$C_j = \frac{\epsilon_s}{W}$

由9,13,14,15消去W \rightarrow

depletion \rightarrow $\frac{C}{C_o} = \frac{1}{\sqrt{1 + \frac{2\epsilon_{ox}^2 V}{qN_A \epsilon_s d^2}}}$ (16)

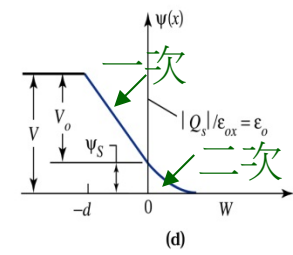
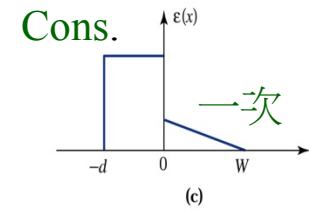
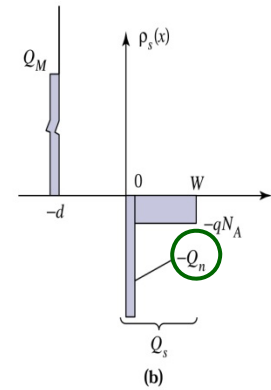
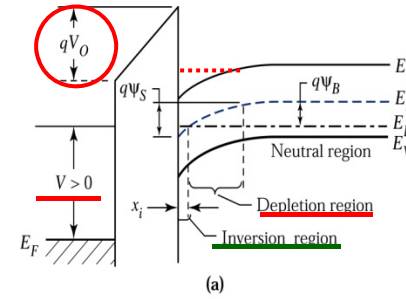
Acc. C=C_{ox} (無C_j)

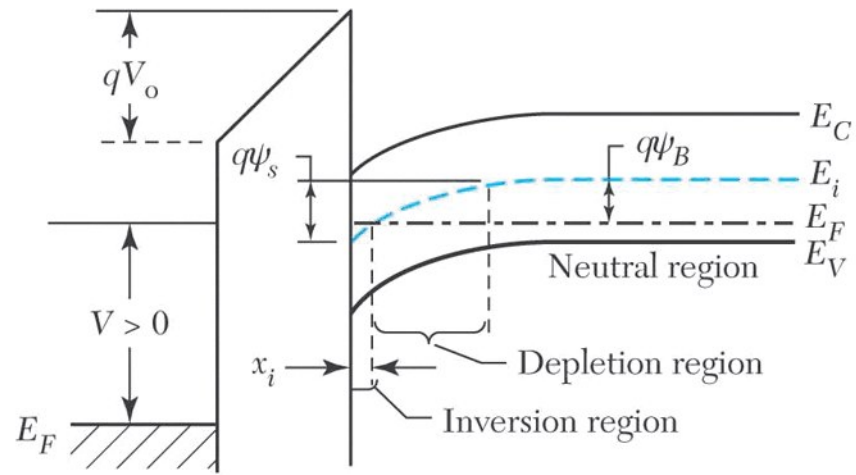
Dep.之 C-V 曲線

最常用之MOS結構 (P-Sub)

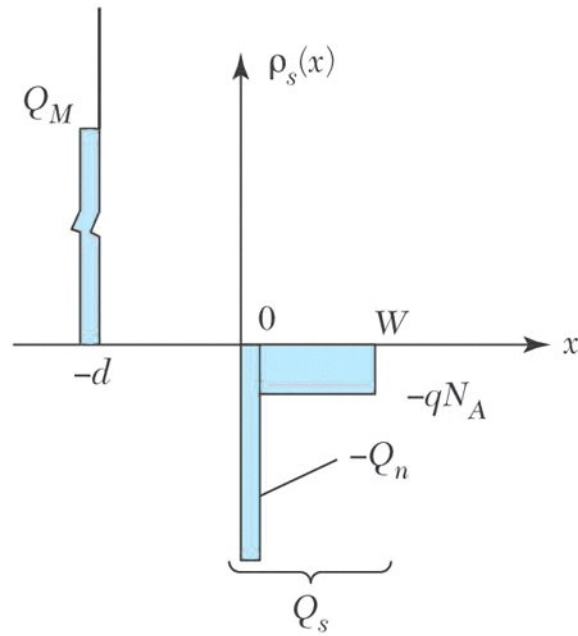
Figure 5.6.

(a) Band diagram of an ideal MOS diode. (b) Charge distributions under inversion condition. (c) Electric-field distribution. (d) Potential distribution.



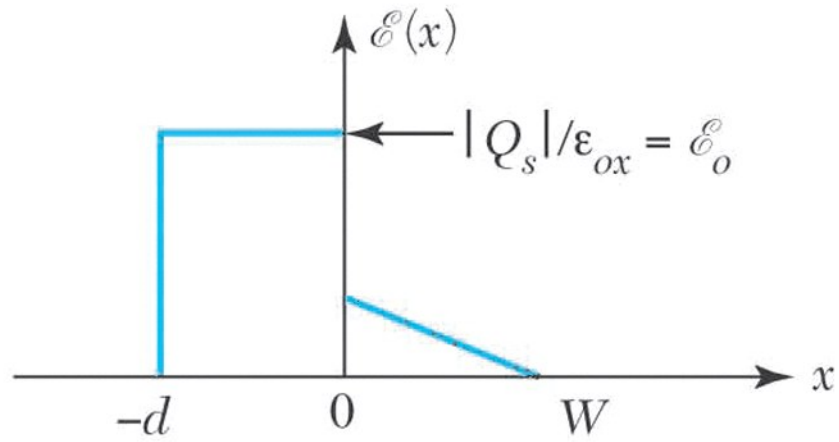


(a)

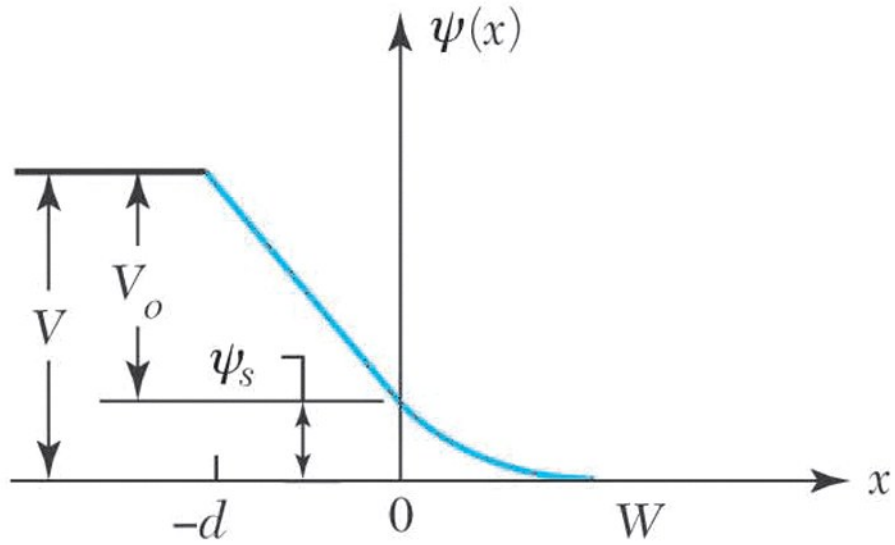


(b)

Figure 5.6ab
© John Wiley & Sons, Inc. All rights reserved.



(c)



(d)

Figure 5.6cd
 © John Wiley & Sons, Inc. All rights reserved.

Threshold
(strong inv. 發生時)

$$V_T = \frac{qN_A W_m}{C_o} + \Psi_s(inv) \cong \frac{\sqrt{2\epsilon_s q N_A (2\Psi_B)}}{C_o} + 2\Psi_B \quad (17)$$

$$C_{min} = \frac{\epsilon_{ox}}{d + (\epsilon_{ox} / \epsilon_s) W_m} \quad \text{不變} \quad (18)$$

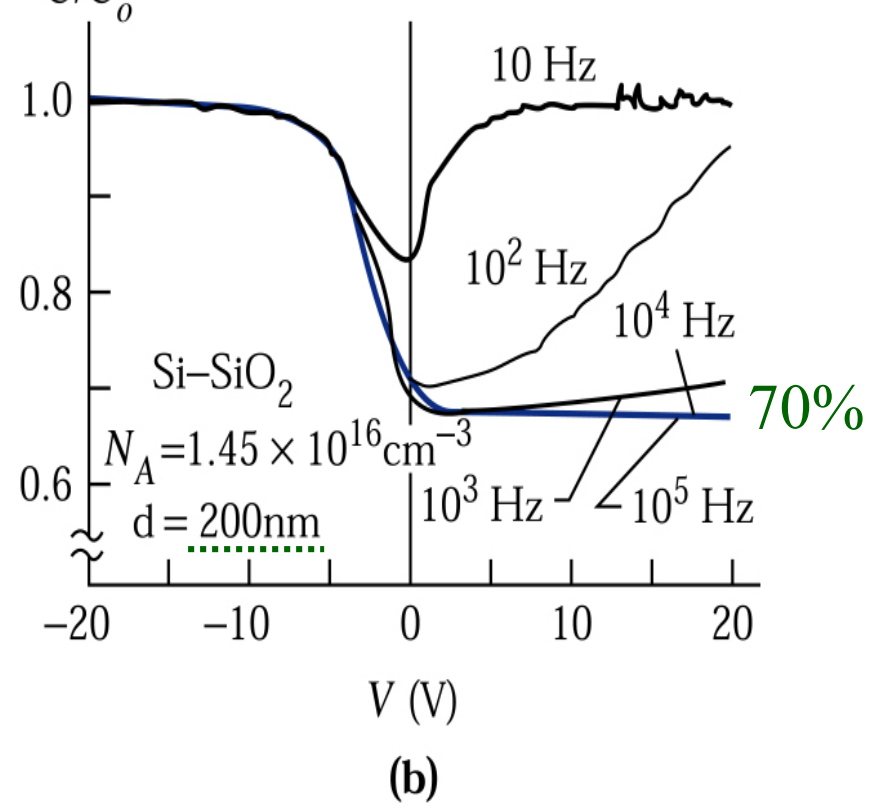
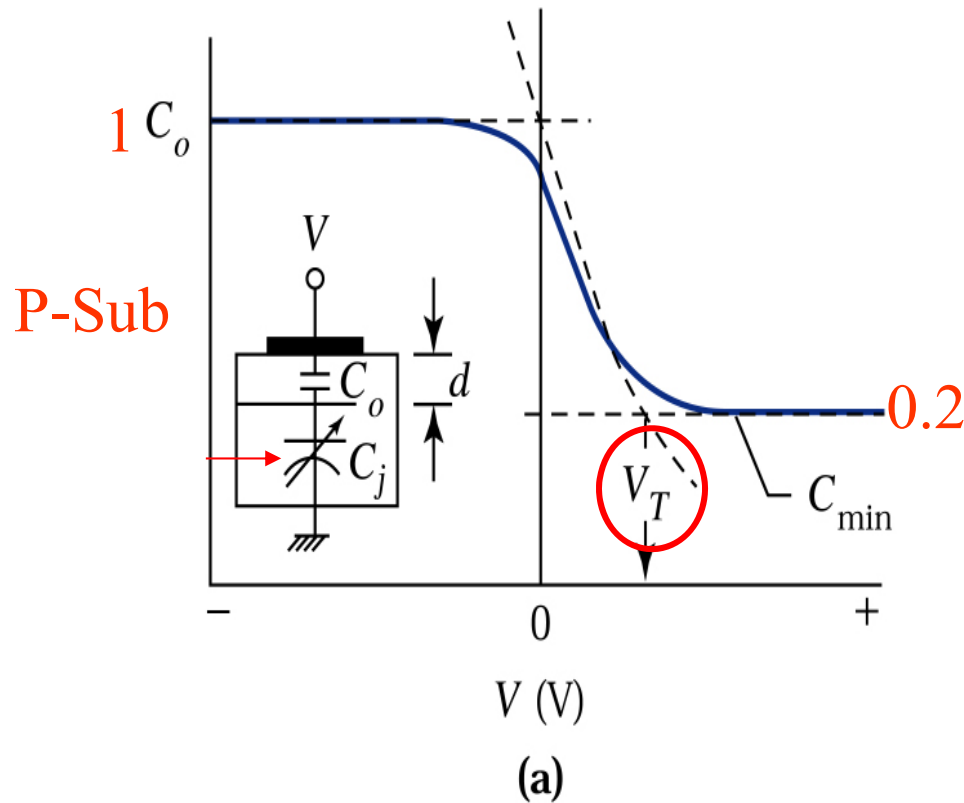


Figure 5.7. (a) High-frequency MOS C-V curve showing its approximated segments (dashed lines). Inset shows the series connection of the capacitors. (b) Effect of frequency on the C-V curve.²

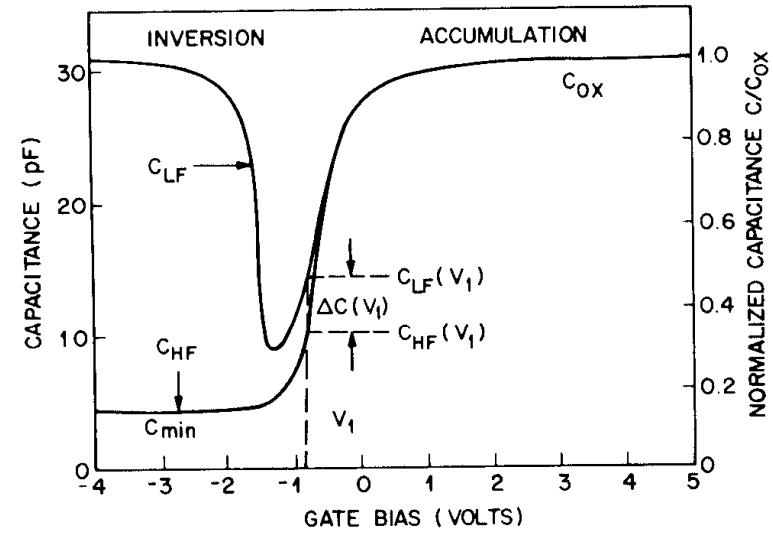
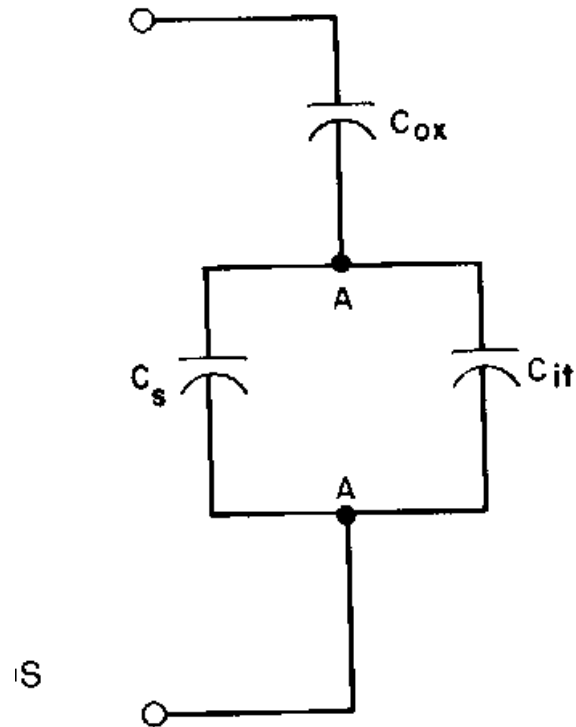


Fig. 8.9 High frequency capacitance C_{HF} and low frequency capacitance C_{LF} as functions of gate bias for an n -type sample illustrating the parameters needed to graphically extract interface trap level density using the high-low frequency capacitance method. After Wagner and Berglund.⁷

$$\frac{1}{C_{LF}} = \frac{1}{C_{ox}} + \frac{1}{C_s + C_{it}}$$

frequency capacitance measured at
fields

$$C_{it} = \left[\frac{1}{C_{LF}} - \frac{1}{C_{ox}} \right]^{-1} - C_s.$$

$$C_s = \left(\frac{1}{C_{HF}} - \frac{1}{C_{ox}} \right)^{-1}.$$

) becomes

$$C_{it} = \left(\frac{1}{C_{LF}} - \frac{1}{C_{ox}} \right)^{-1} - \left(\frac{1}{C_{HF}} - \frac{1}{C_{ox}} \right)^{-1}.$$

$$\underline{C_{LF} = \Delta C + C_{HF}} \quad (8.23)$$

$\Delta C = C_{LF} - C_{HF}$. Substituting (8.23) into (8.22) yields

$$\begin{aligned} \underline{D_{it}} &= \frac{C_{ox}}{q} \left[\left(\frac{1}{\Delta C/C_{ox} + C_{HF}/C_{ox}} - 1 \right)^{-1} - \left(\frac{1}{C_{HF}/C_{ox}} - 1 \right)^{-1} \right] \\ &= \frac{\Delta C}{q} \left(1 - \frac{C_{HF} + \Delta C}{C_{ox}} \right)^{-1} \left(1 - \frac{C_{HF}}{C_{ox}} \right)^{-1} \end{aligned} \quad (8.24)$$

λ_{it} is related to D_{it} by (8.13). Equation (8.24) from Wagner λ_{it}^7 is plotted in Fig. 8.8 with

$$D_{it} = D_{ito} \frac{1000}{x_o} \quad (8.25)$$

Problem

For an ideal metal-SiO₂-Si diode having $N_A = 10^{16} \text{ cm}^{-3}$ and $d = 250 \text{ \AA}$, calculate the minimum capacitance on the C - V curve of Fig. 27a. The relative dielectric constant of SiO₂ is 3.9.

Solution

$$C_o = \frac{\epsilon_{ox}}{d} = \frac{3.9 \times (8.85 \times 10^{-14})}{250 \times 10^{-8}} = 1.38 \times 10^{-7} \text{ F/cm}^2$$

$$Q_{sc} = -qN_A W_m = -1.6 \times 10^{-19} \times 10^{16} \times (3 \times 10^{-5}) = -4.8 \times 10^{-8} \text{ C/cm}^2.$$

We used Fig. 25 for W_m ;

$$\psi_s(\text{inv}) = 2\psi_B = \frac{2kT}{q} \ln \left[\frac{N_A}{n_i} \right] = 0.69 \text{ V}$$

$$V_T = -\frac{Q_{sc}}{C_o} + 2\psi_B = 0.35 + 0.69 = 1.04 \text{ V}.$$

The minimum capacitance C_{\min} at V_T is

$$\begin{aligned} C_{\min} &= \frac{\epsilon_{ox}}{d + (\epsilon_{ox}/\epsilon_s)W_m} = \frac{3.9 \times (8.85 \times 10^{-14})}{2.5 \times 10^{-6} + (3.9/11.9)3 \times 10^{-5}} \\ &= 2.8 \times 10^{-8} \text{ F/cm}^2. \end{aligned}$$

Therefore, C_{\min} is about 20% of C_o .

Figure 5.8.

Work function difference as a function of background impurity concentration for Al, n^+ -, and p^+ polysilicon gate materials.

Ideal $q\Phi_{ms} = 0$

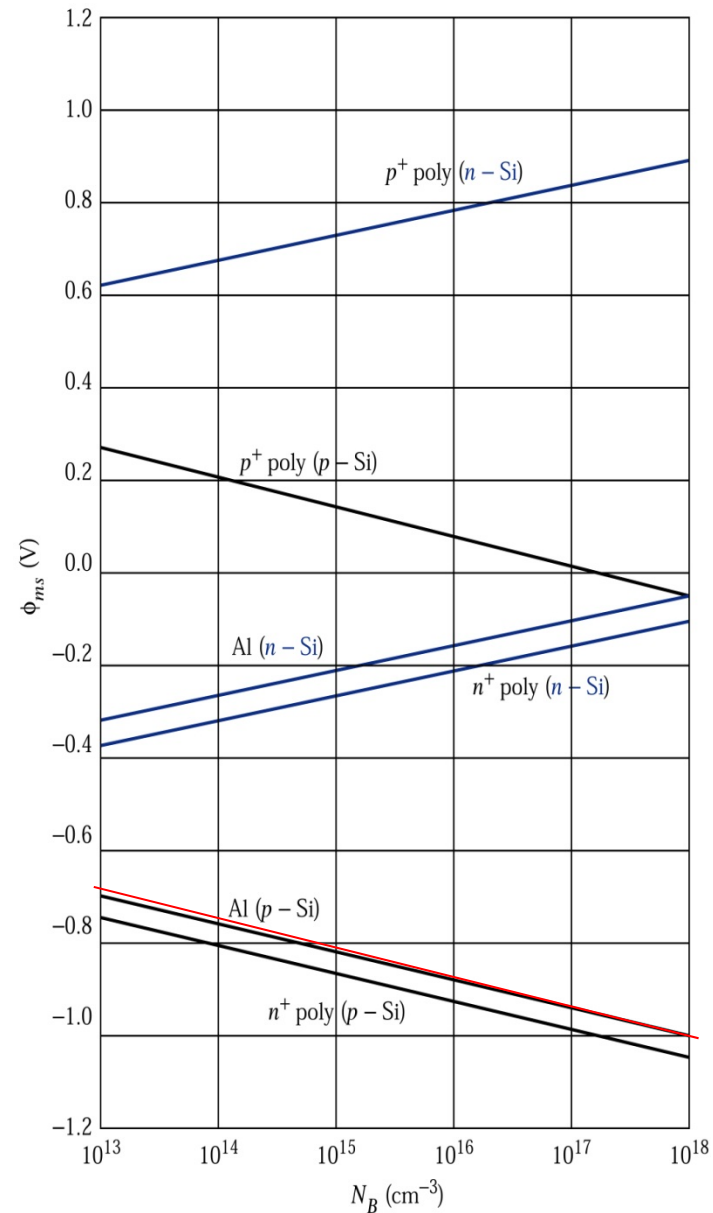
$q\Phi_{ms} = q\Phi_m - q\Phi_s$

Al: $q\Phi_m = 4.1\text{eV}$

n^+ -poly: $q\Phi_m = 3.95\text{eV}$

通常為負

P-Sub, 負更多



$$V_{FB} = \frac{q\Phi_{ms}}{q} = \Phi_m - \Phi_s$$

Flat-band (在Si), 定義 $\Psi_s=0$

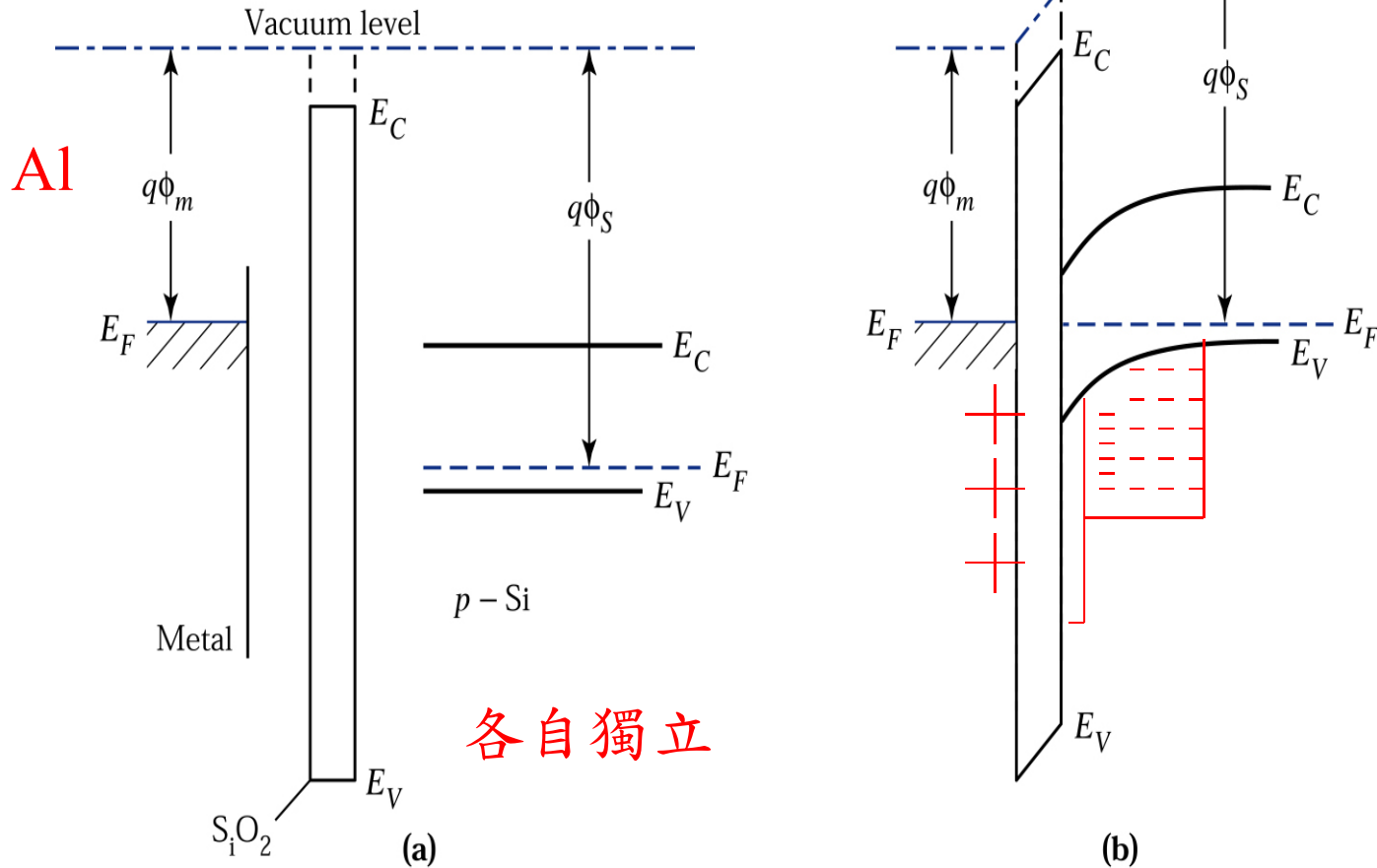


Figure 5.9. (a) Energy band diagram of an isolated metal and an isolated semiconductor with an oxide layer between them. (b) Energy band diagram of an MOS diode in thermal equilibrium.

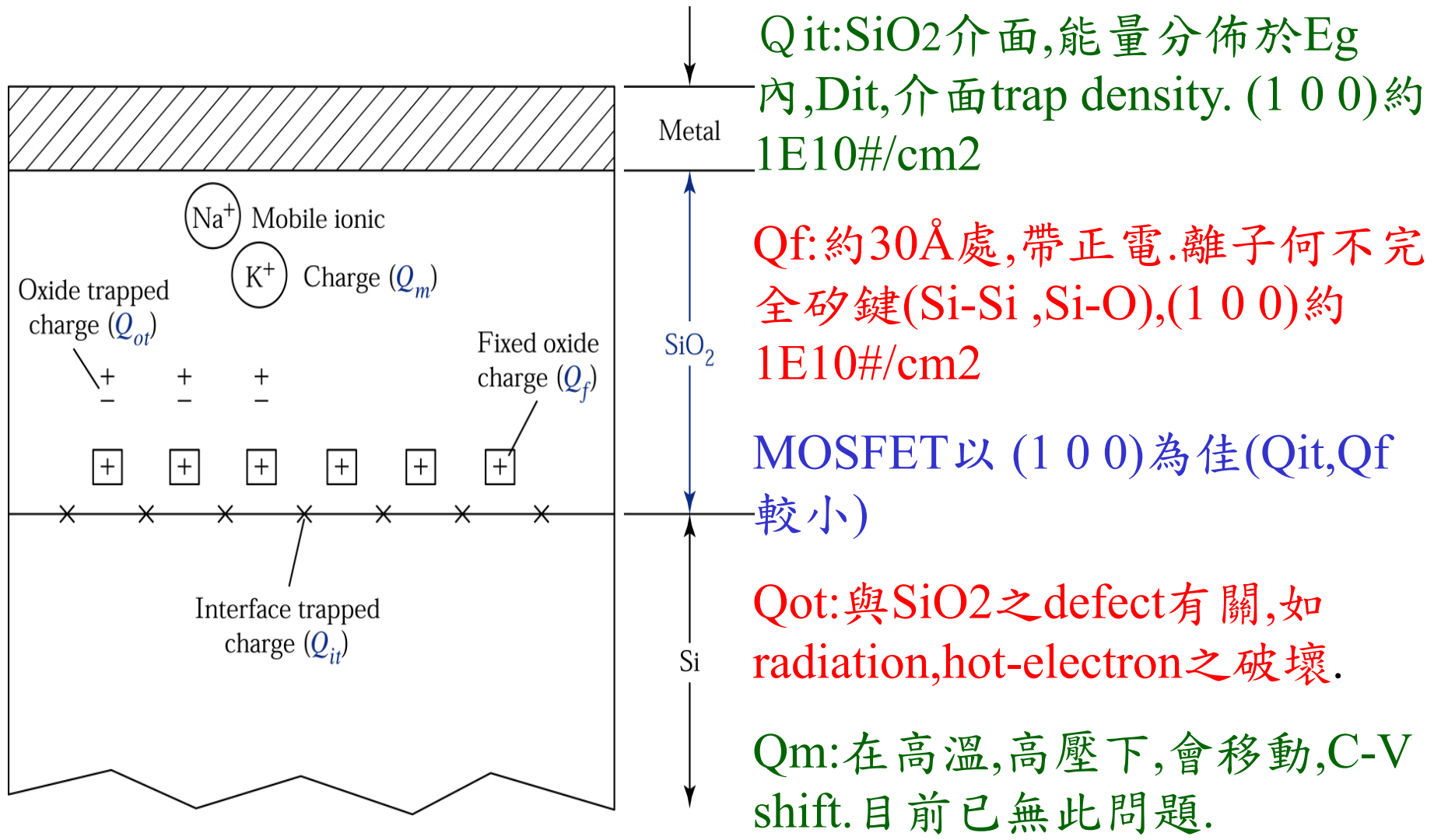
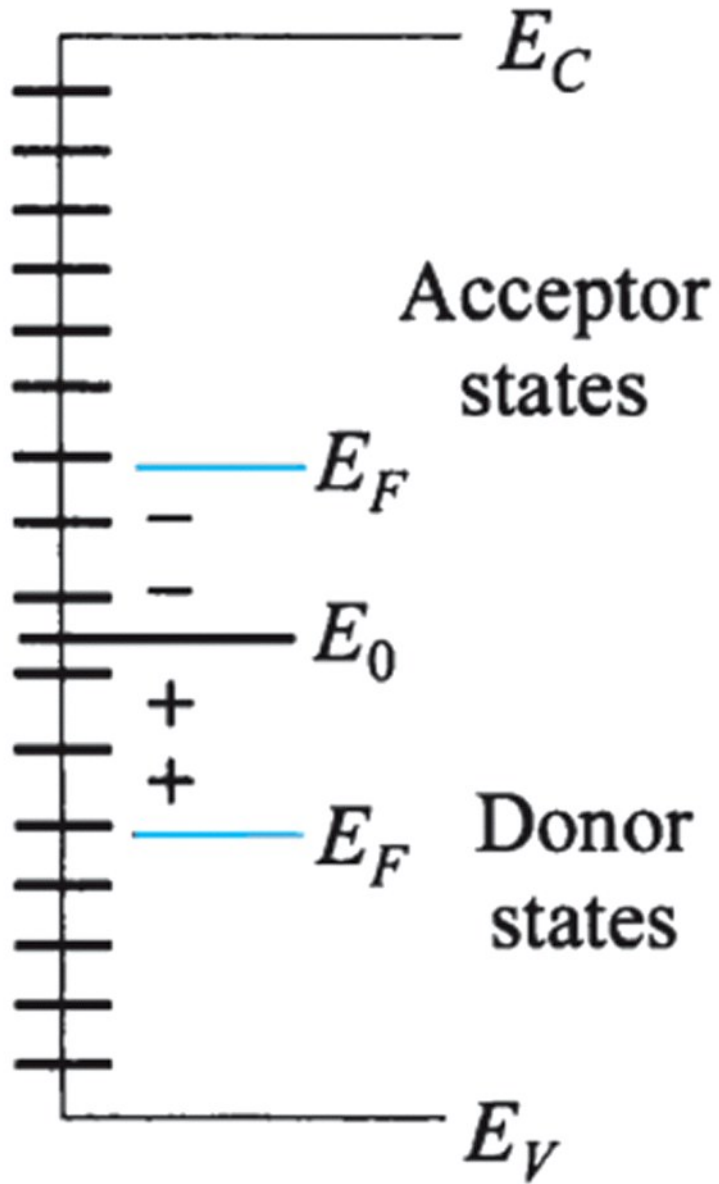


Figure 5.10. Terminology for the charges associated with thermally oxidized silicon.³



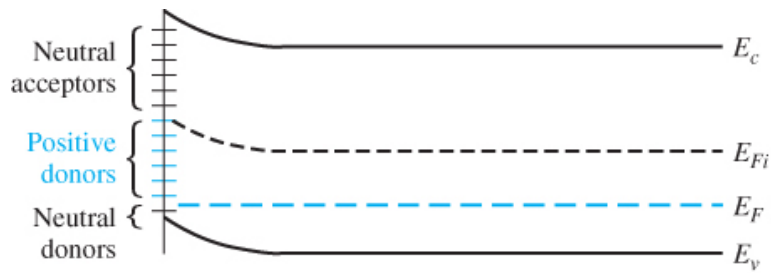
In general, **acceptor states exist in the upper half of the bandgap** and **donor states exist in the lower half of the bandgap.**

An acceptor state is neutral if the Fermi level is below the state and becomes negatively charged if the Fermi level is above the state.

A donor state is neutral if the Fermi level is above the state and becomes positively charged if the Fermi level is below the state.

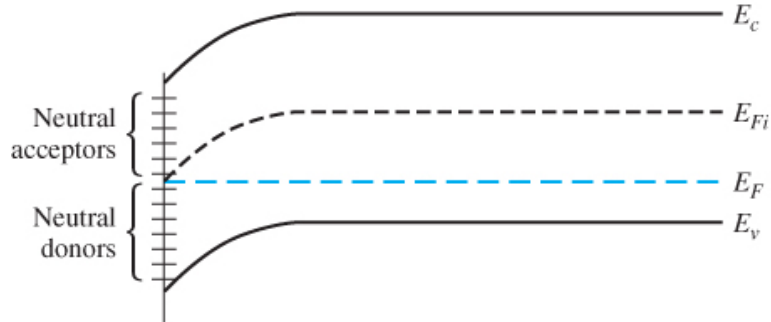
The charge of the interface states is then a function of the gate voltage applied across the MOS capacitor.

Figure 5.11
 © John Wiley & Sons, Inc. All rights reserved.

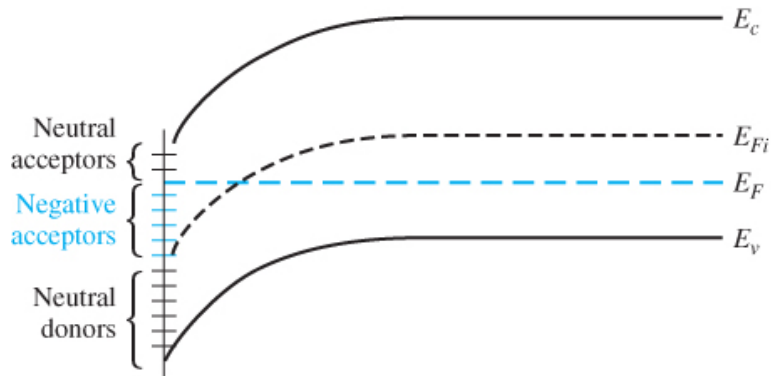


(a)

there is a net positive charge trapped in the donor states.



(b)



(c)

there is now a net negative charge in the acceptor states.

Figure 10.32 | Energy-band diagram in a p-type semiconductor showing the charge trapped in the interface states when the MOS capacitor is biased (a) in accumulation, (b) at midgap, and (c) at inversion.

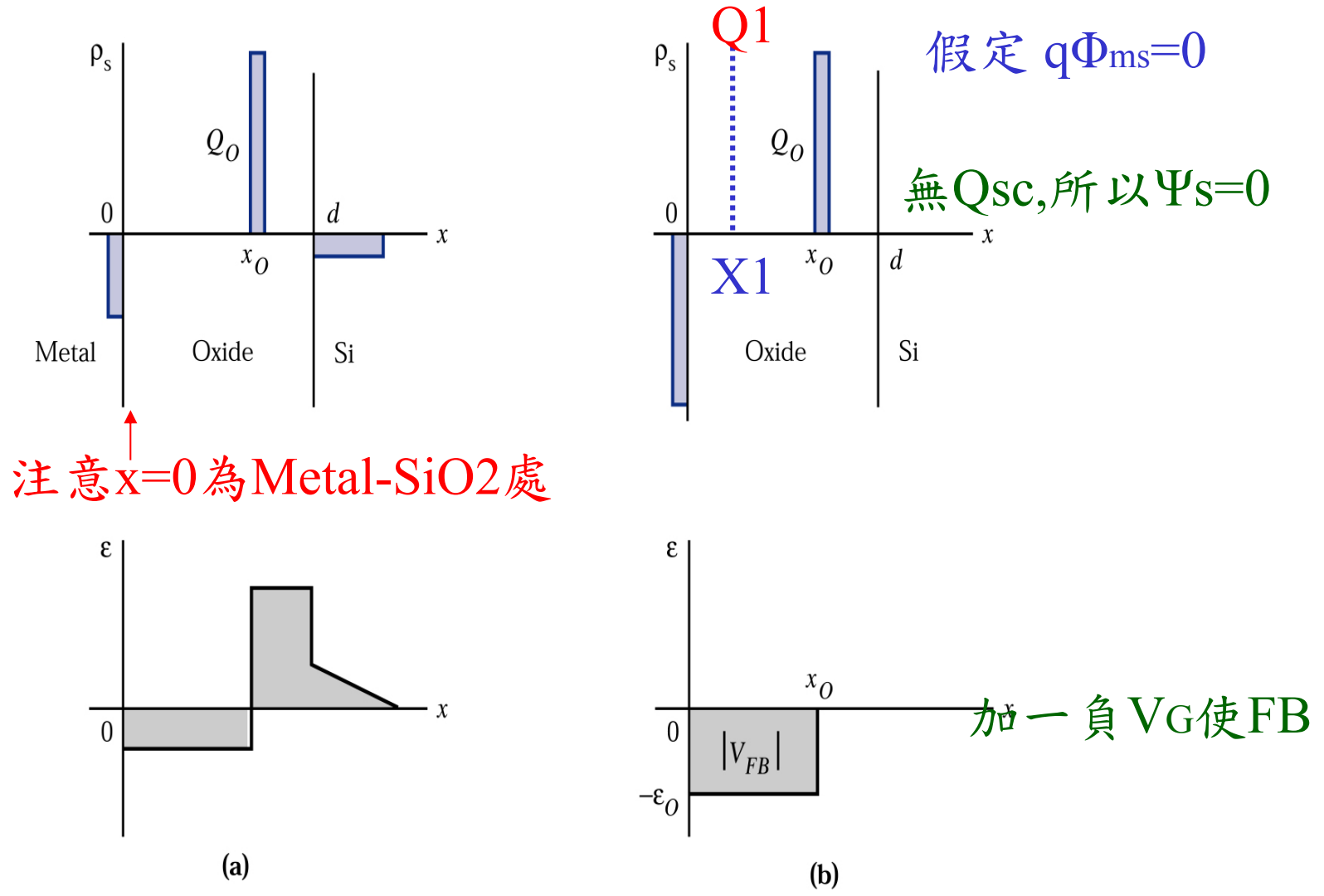


Figure 5.12. Effect of a sheet charge within the oxide.² (a) Condition for $V_G = 0$. (b) Flat-band condition.

Q_o :單位面積電荷, C_o :單位面積電容

$$V_{FB} = - \mathcal{E}_o x_o = - \frac{Q_o}{\epsilon_{ox}} x_o = - \frac{Q_o}{C_o} \frac{x_o}{d} \quad (19)$$

當 Q_o 接近SiO₂/Si時 ($X_o=d$)

$$V_{FB} = - \frac{Q_o}{C_o} \left[\frac{d}{d} \right] = - \frac{Q_o}{C_o} \quad (20)$$

若 Q_o 任意分布

$$V_{FB} = - \frac{1}{C_o} \left[\frac{1}{d} \int_0^d \overset{X_o}{x} \overset{Q_o}{\rho(x)} dx \right] \quad (21)$$

$\rho(x)$: volume charge density

得知 $\rho_{ot}(x)$, $\rho_m(x)$,可求出 Q_{ot} , Q_m 對 V_{FB} 之影響

$$\left\{ \begin{array}{l} Q_{ot} \equiv \frac{1}{d} \int_0^d x \rho_{ot}(x) dx \quad (22a) \\ Q_m \equiv \frac{1}{d} \int_0^d x \rho_m(x) dx \quad (22b) \end{array} \right.$$

(若 Q 為正, V_G 須加負)

$$V_{FB} = \phi_{ms} - \frac{Q_f + Q_m + Q_{ot}}{C_o} \cdot +Q_{it}/C_{ox} \quad (23)$$

無 Q 時, $V_{FB}=\Phi_{ms}$

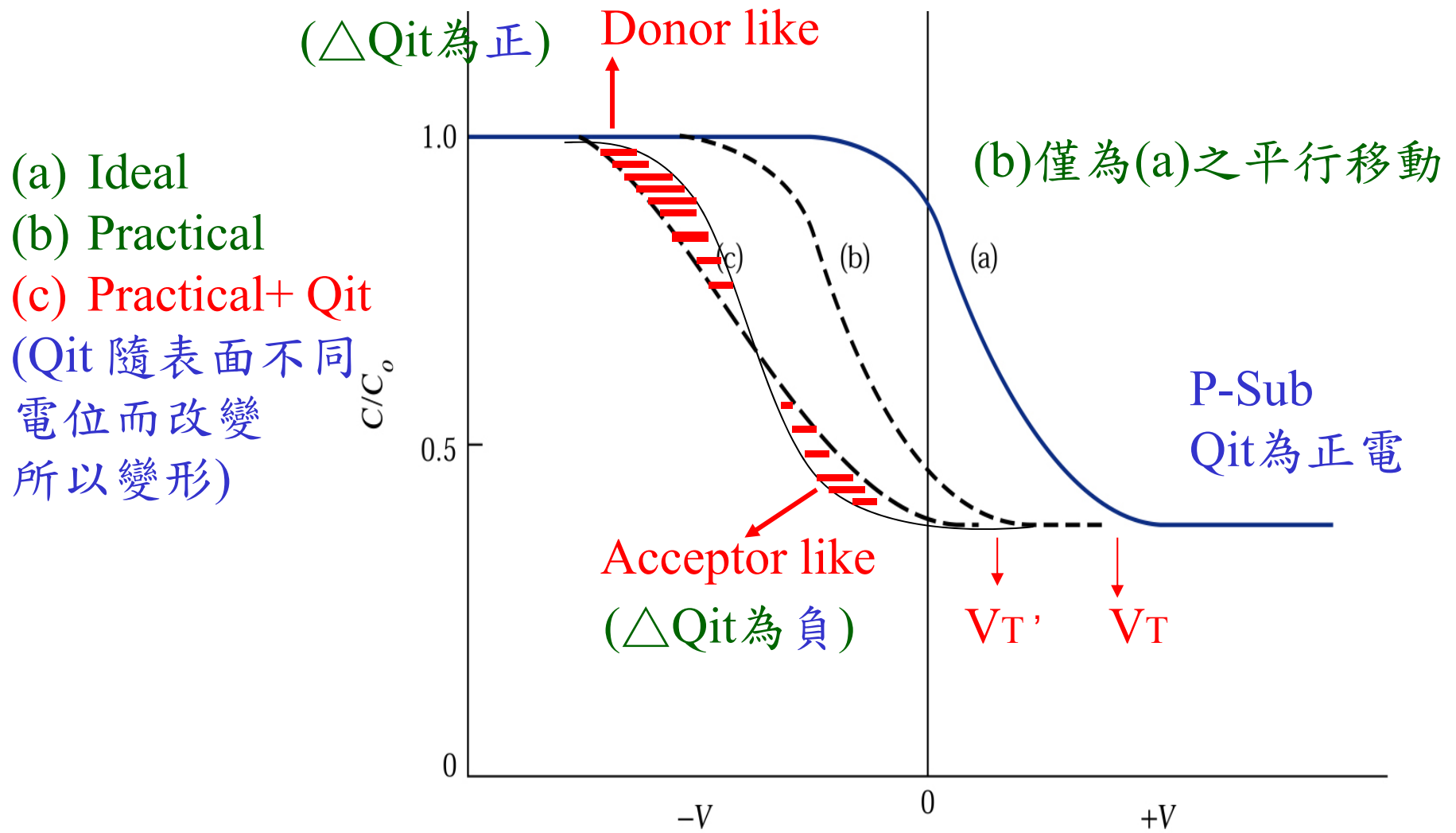
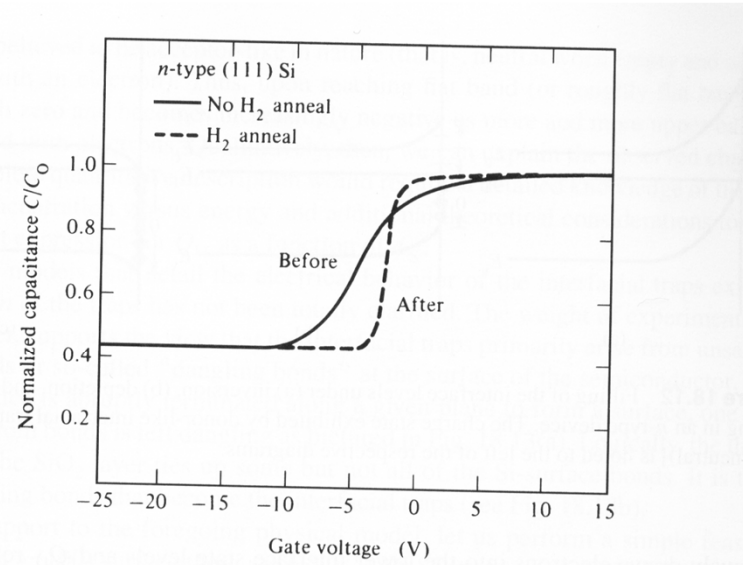


Figure 5.13. Effect of a fixed oxide charge and interface traps on the C-V characteristics of an MOS diode.



C-V characteristics derived from the same MOS-C before () and after ()

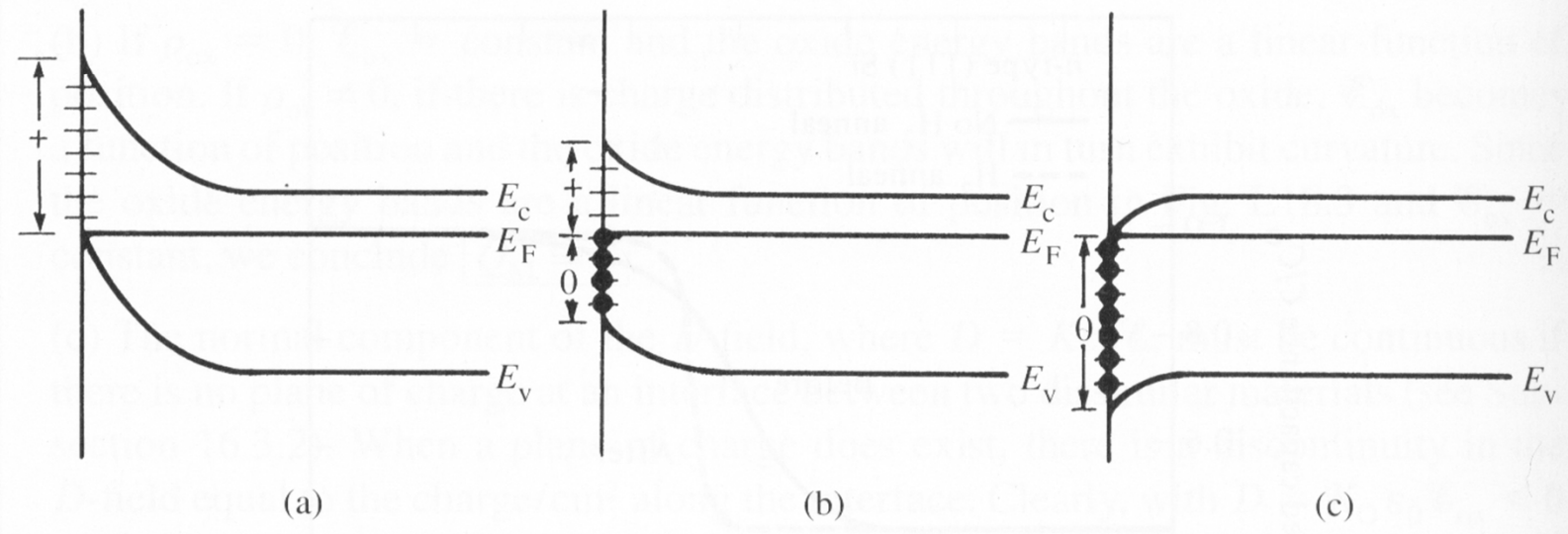


Figure 18.12 Filling of the interface levels under (a) inversion, (b) depletion, and (c) accumulation biasing in an *n*-type device. The charge state exhibited by donor-like interfacial traps [“+” (plus) or “0” (neutral)] is noted to the left of the respective diagrams.

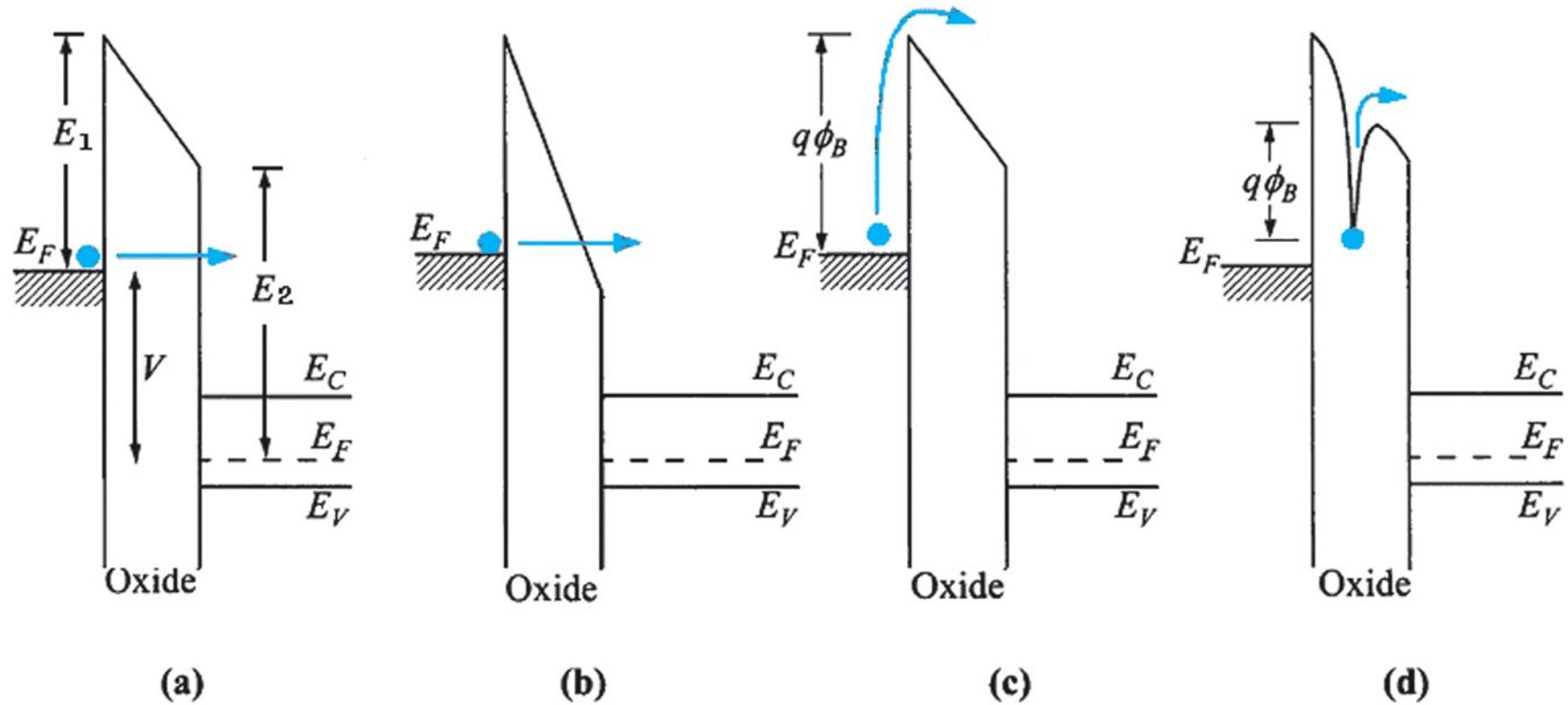


Figure 5.14
 © John Wiley & Sons, Inc. All rights reserved.

Conduction mechanisms in MOS,
 (a) Direct tunneling (b) Fowler-Nordheim tunneling
 (c) Thermionic emission (d) Frenkel-Poole emission

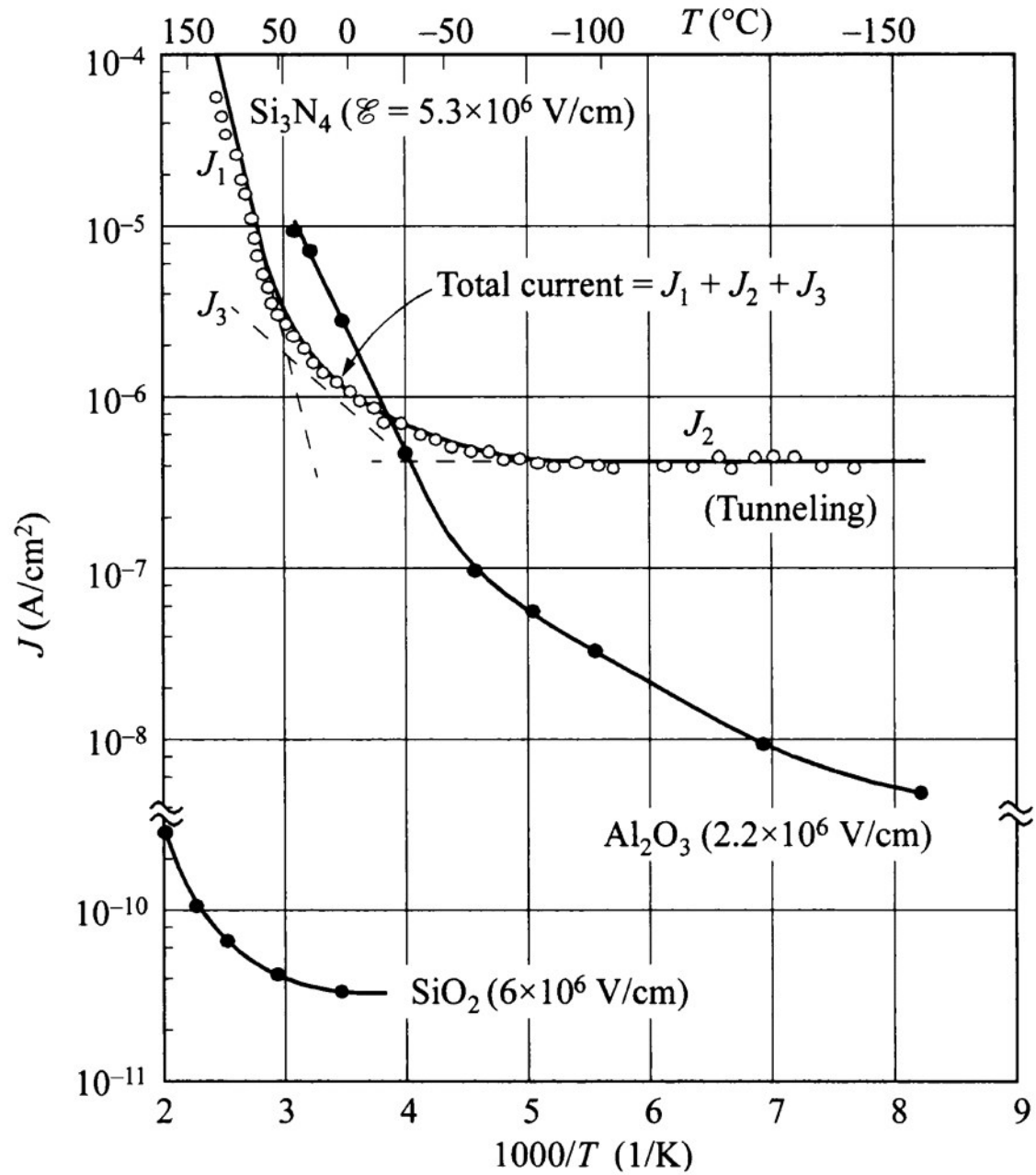


Figure 5.15
 © John Wiley & Sons, Inc. All rights reserved.

Dielectric Breakdown

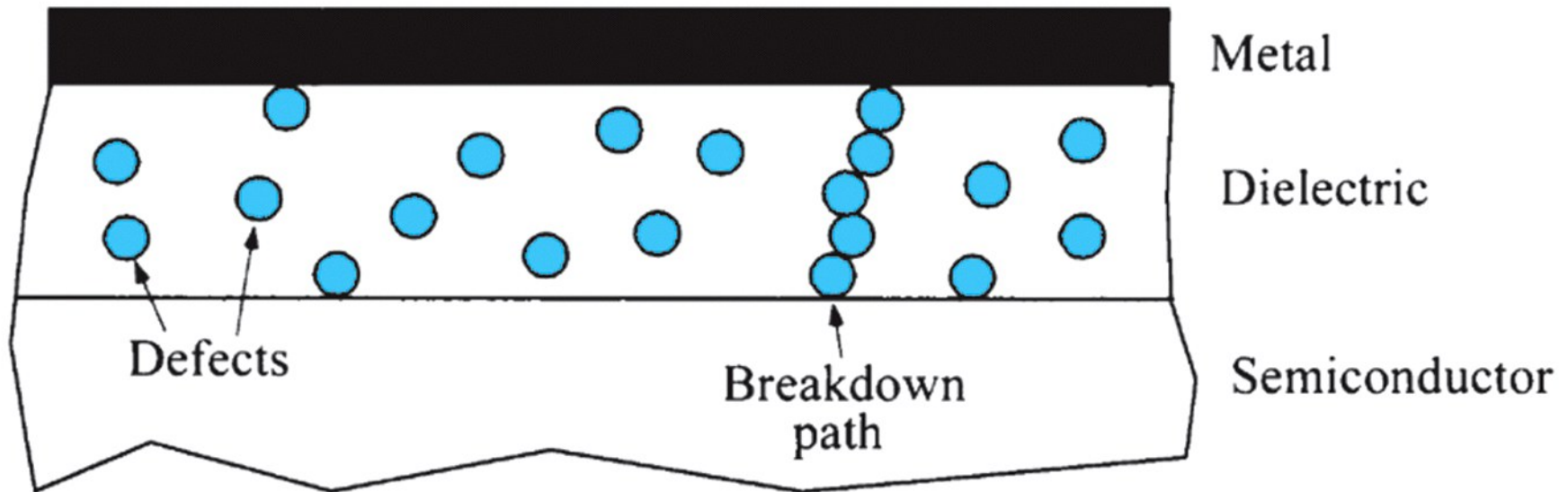


Figure 5.16
© John Wiley & Sons, Inc. All rights reserved.

Percolation theory

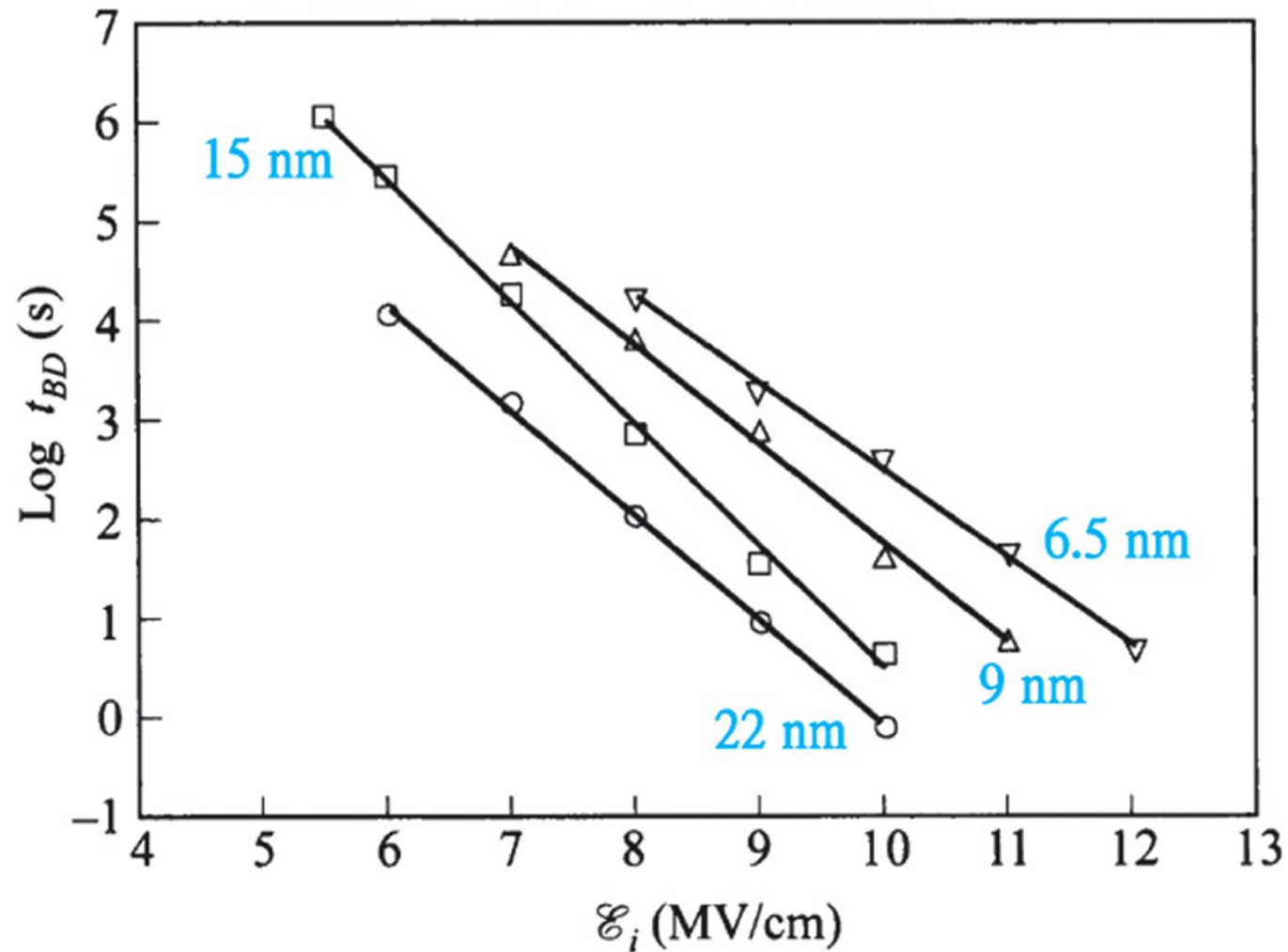
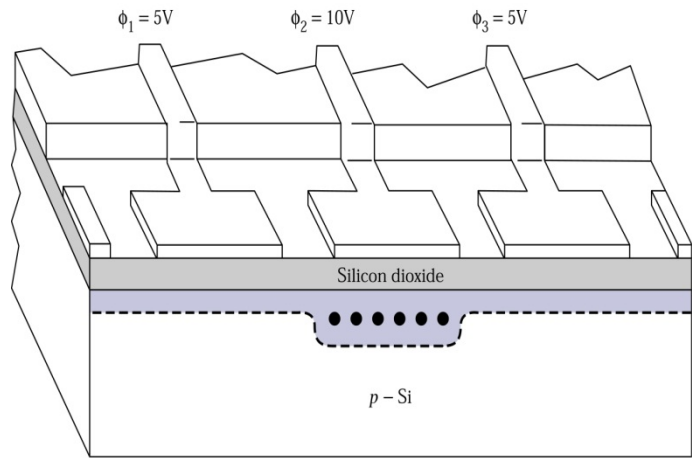
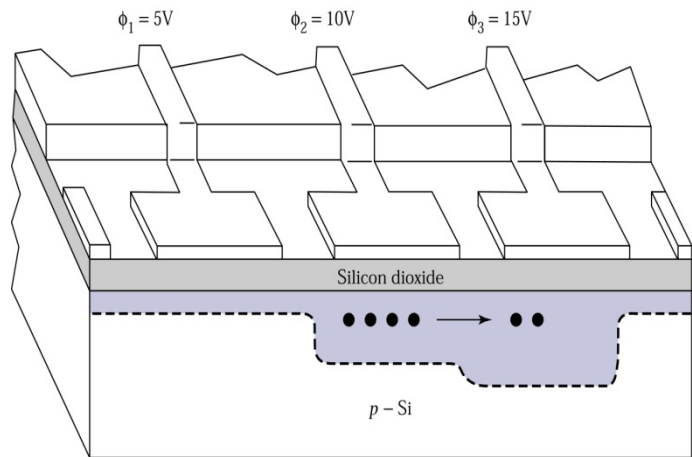


Figure 5.17
 © John Wiley & Sons, Inc. All rights reserved.

Time to breakdown vs oxide field for various thicknesses



(a)



(b)

Image sensing
Signal processing

Figure 5.18. Cross section of a three-phase charge-coupled device.⁴
 (a) High voltage on ϕ_2 . (b) ϕ_3 pulsed to a higher voltage for charge transfer.

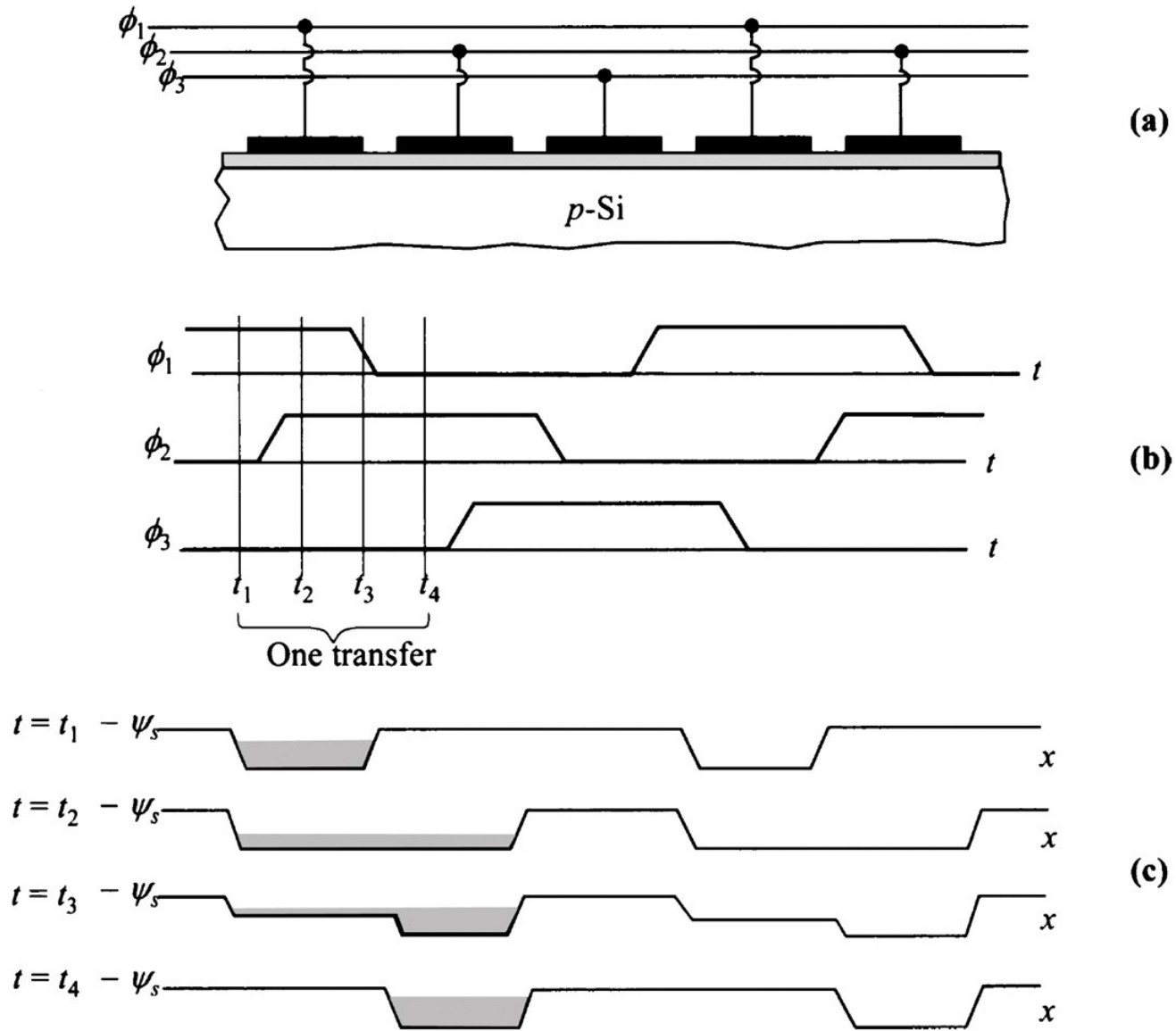


Figure 5.19
 © John Wiley & Sons, Inc. All rights reserved.

CCD charge transfer, (a) three-phase gate bias, (b)clock

Readout mechanisms,

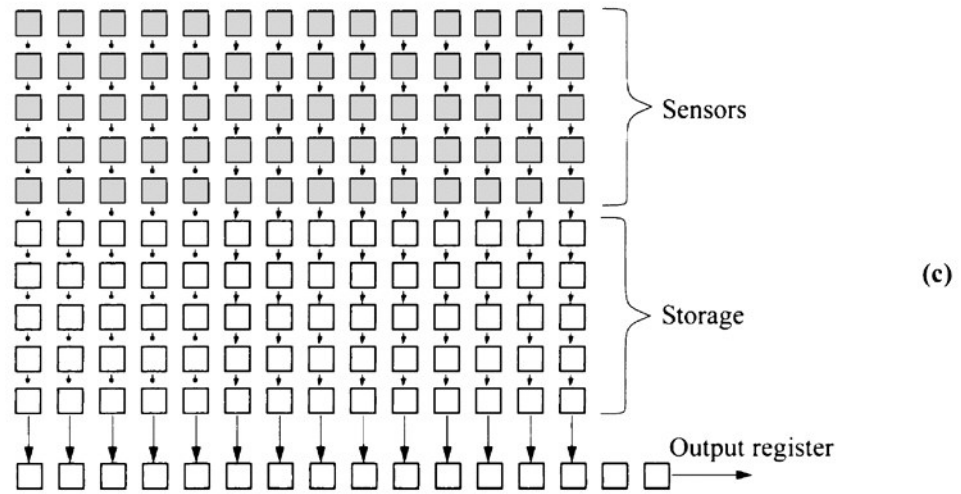
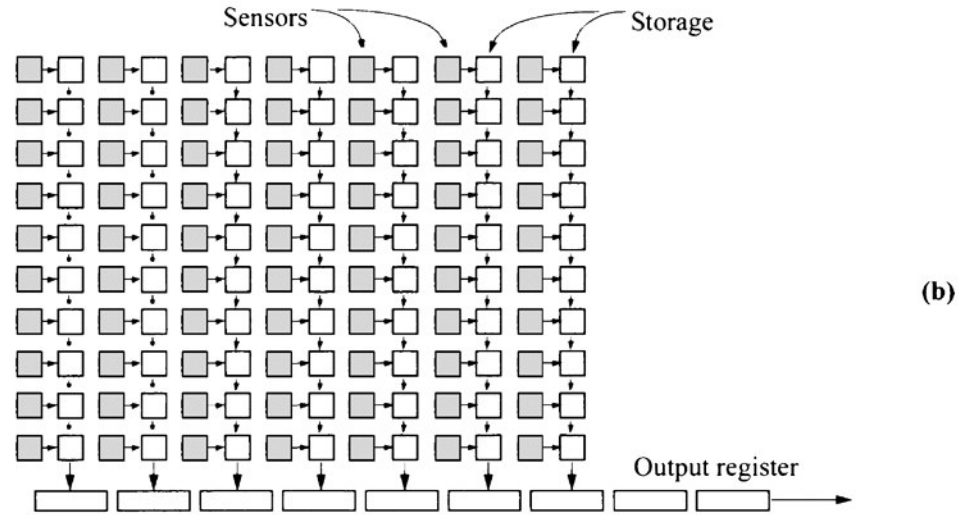
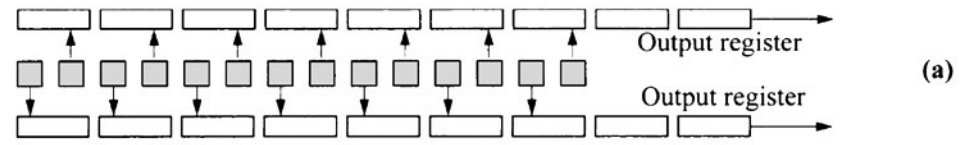
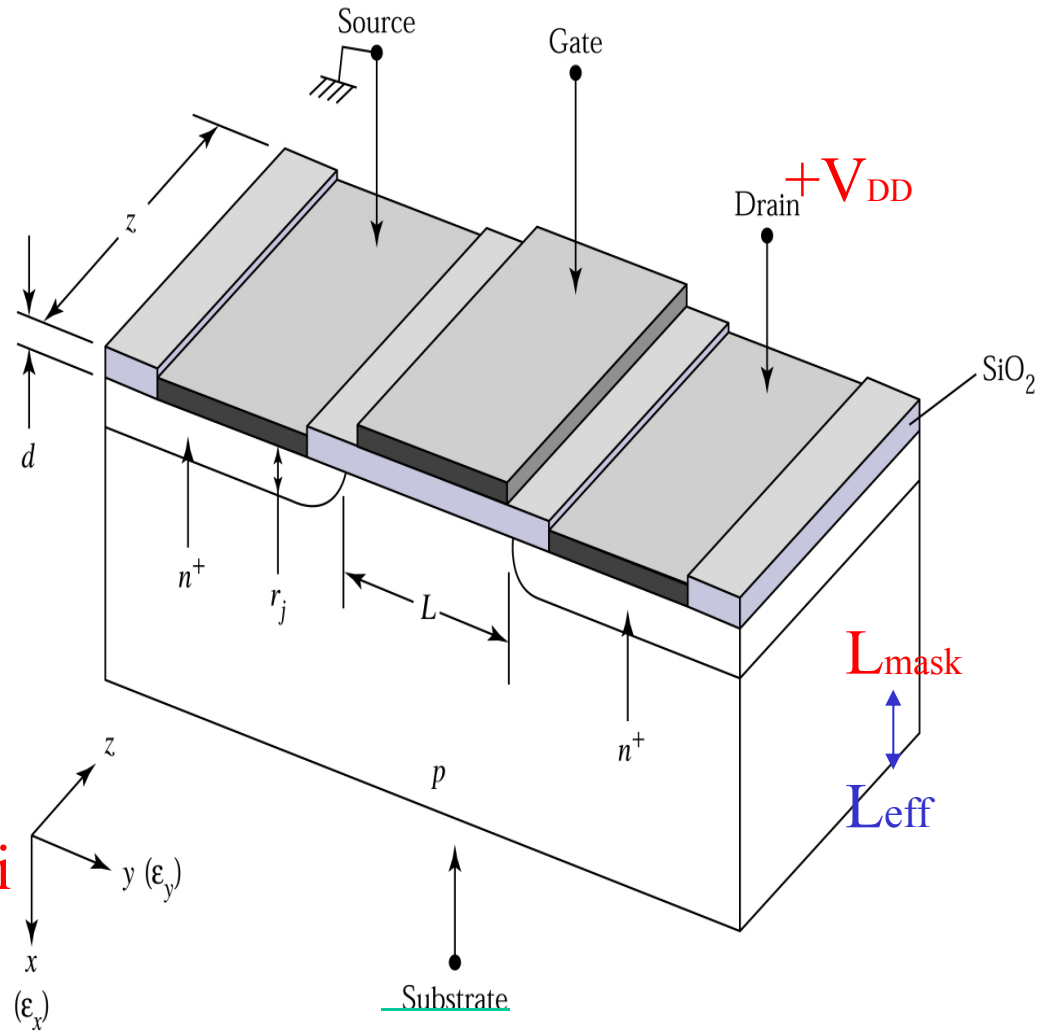


Figure 5.20
© John Wiley & Sons, Inc. All rights reserved.

- * 為4-terminal
- * L 為D到S之長度
(與Gate無關)
- * 中間部分,
即為MOS capacitor



- * Gate 為 poly-Si, silicide/poly-Si
(n+) (n+)
- * S, D 為 n+/p junction

Figure 5.21. Perspective view of a metal-oxide-semiconductor field-effect transistor (MOSFET).

Given, fixed V_G 下

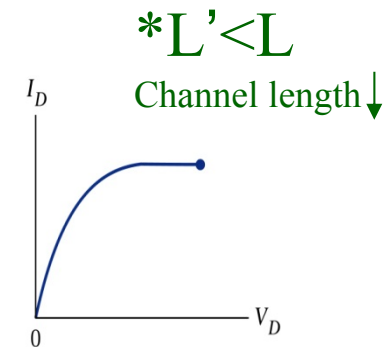
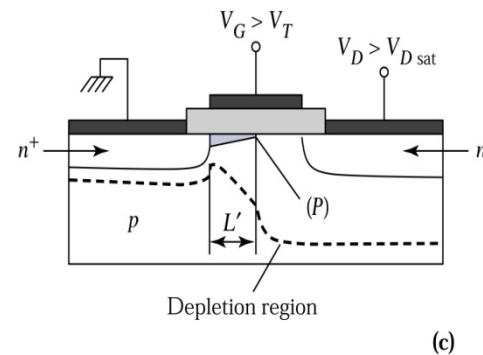
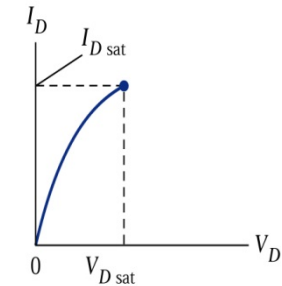
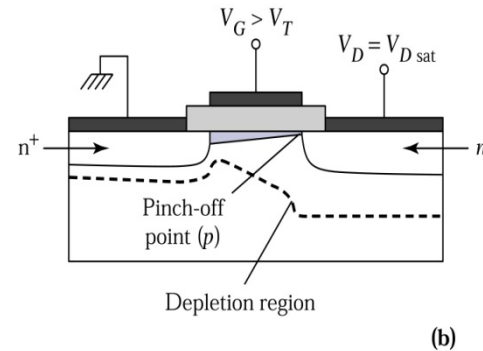
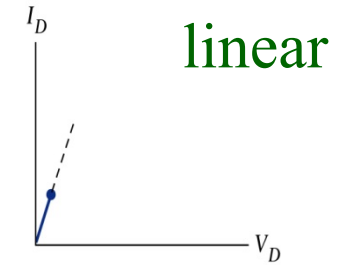
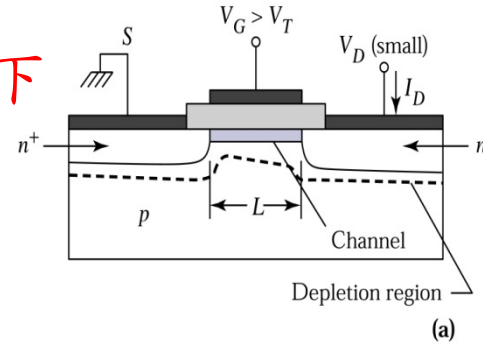
Figure 5.22.

Operations of the MOSFET and output I - V characteristics.

(a) Low drain voltage.

(b) Onset of saturation. Point P indicates the pinch-off point.

(c) Beyond saturation.



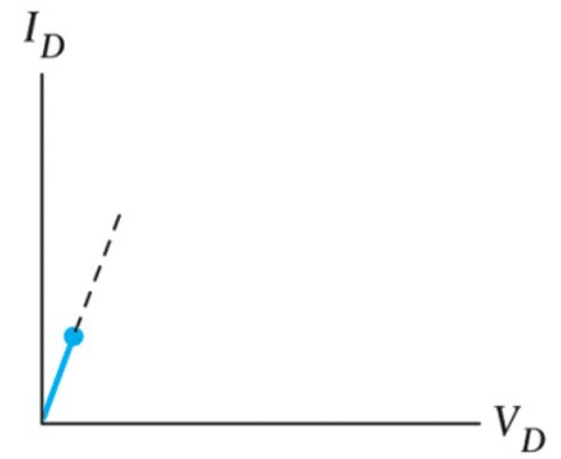
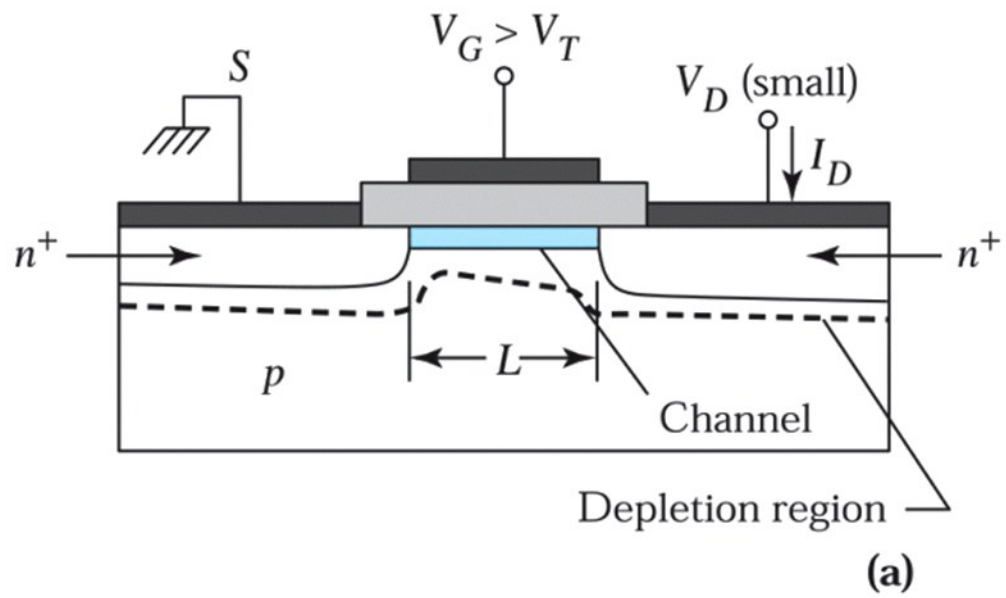
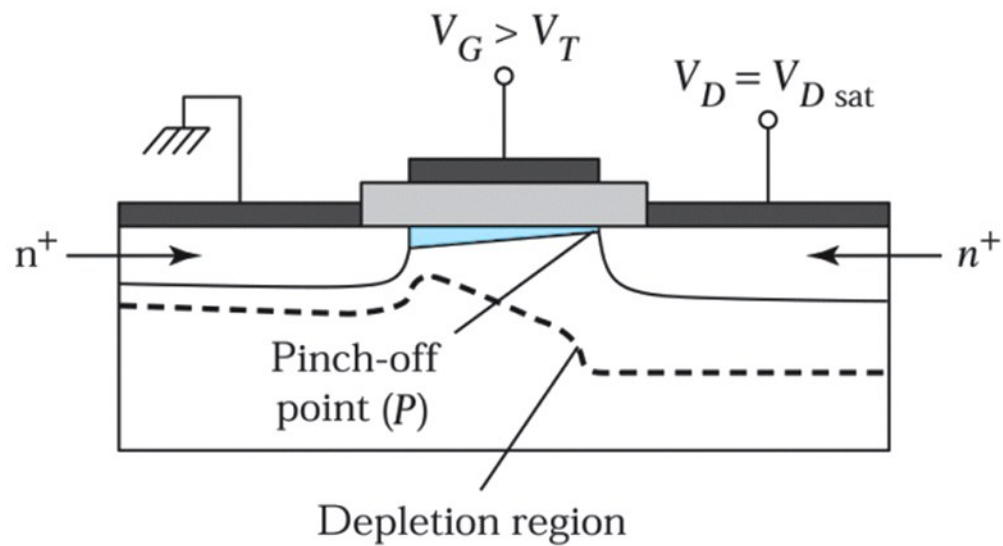


Figure 5.22a
 © John Wiley & Sons, Inc. All rights reserved.



(b)

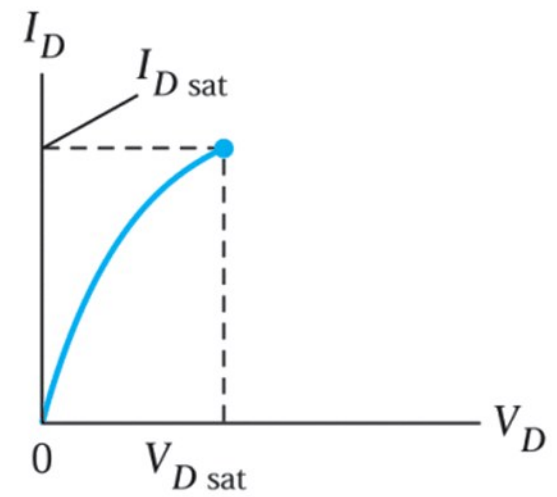
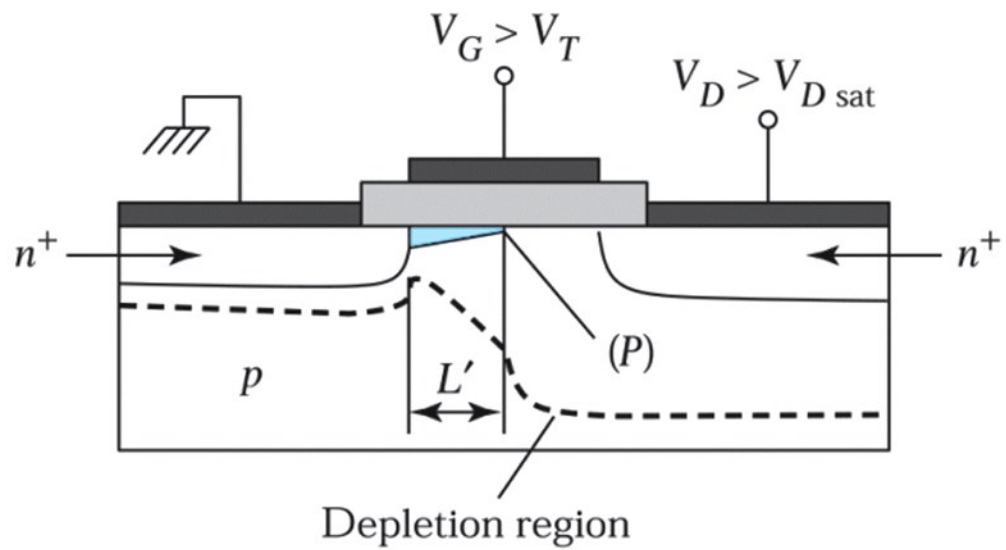


Figure 5.22b
 © John Wiley & Sons, Inc. All rights reserved.



(c)

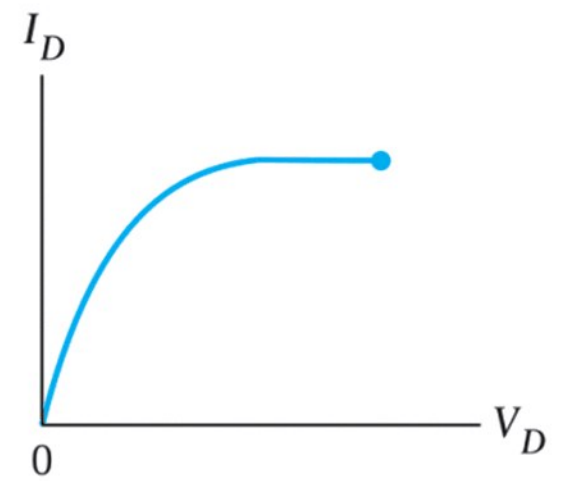


Figure 5.22c
 © John Wiley & Sons, Inc. All rights reserved.

以下推導 I_0 vs V_D 之 general eq.

參考 Fig.16

$$Q_s(y) = -[V_G - \psi_s(y)]C_o \quad (-Q_s/C_o = V_o) \quad (24)$$

感應在半導體內, 單位面積電荷

$$Q_n(y) = Q_s(y) - Q_{sc}(y) = -[V_G - \psi_s(y)]C_o - Q_{sc}(y). \quad (25)$$

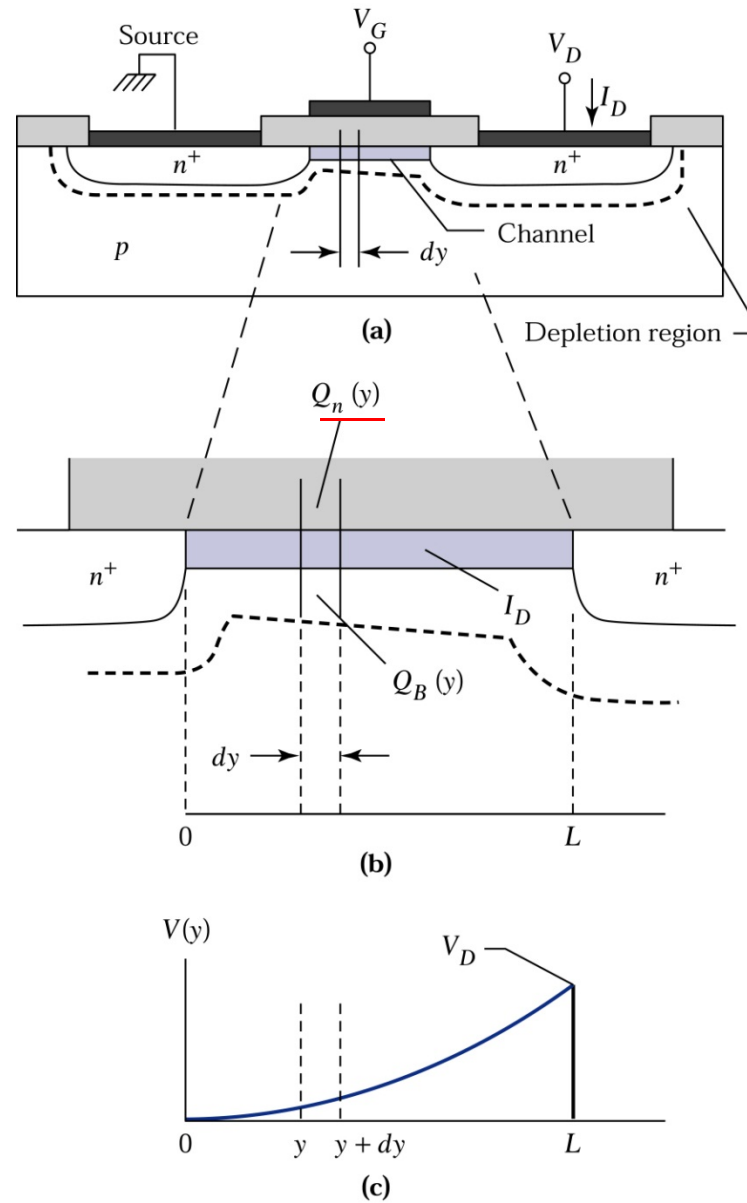
\therefore inv. $\Psi_s(y) \sim 2\phi_B + V(y)$

$$Q_{sc}(y) = -qN_A W_m \simeq -\sqrt{2\epsilon_s q N_A [V(y) + 2\psi_B]}. \quad (26)$$

Figure 5.23.

(a) MOSFET operated in the **linear** region.

(b) Enlarged view of the channel. (c) **Drain voltage drop** along the channel.



$$Q_n(y) \simeq -[V_G - V(y) - 2\psi_B]C_0 + \sqrt{2\epsilon_s q N_A [V(y) + 2\psi_B]}. \quad (27)$$

$$\sigma(x) = qn(x)\mu_n(x). \quad (28) \quad \text{p.53 (14)}$$

$$g = \frac{Z}{L} \int_0^{x_i} \sigma(x) dx = \frac{Z\mu_n}{L} \int_0^{x_i} qn(x) dx. \quad (29)$$

$$g = \frac{Z\mu_n}{L} |Q_n|. \quad (30)$$

$\rightarrow dy/dR = L/(1/g)$

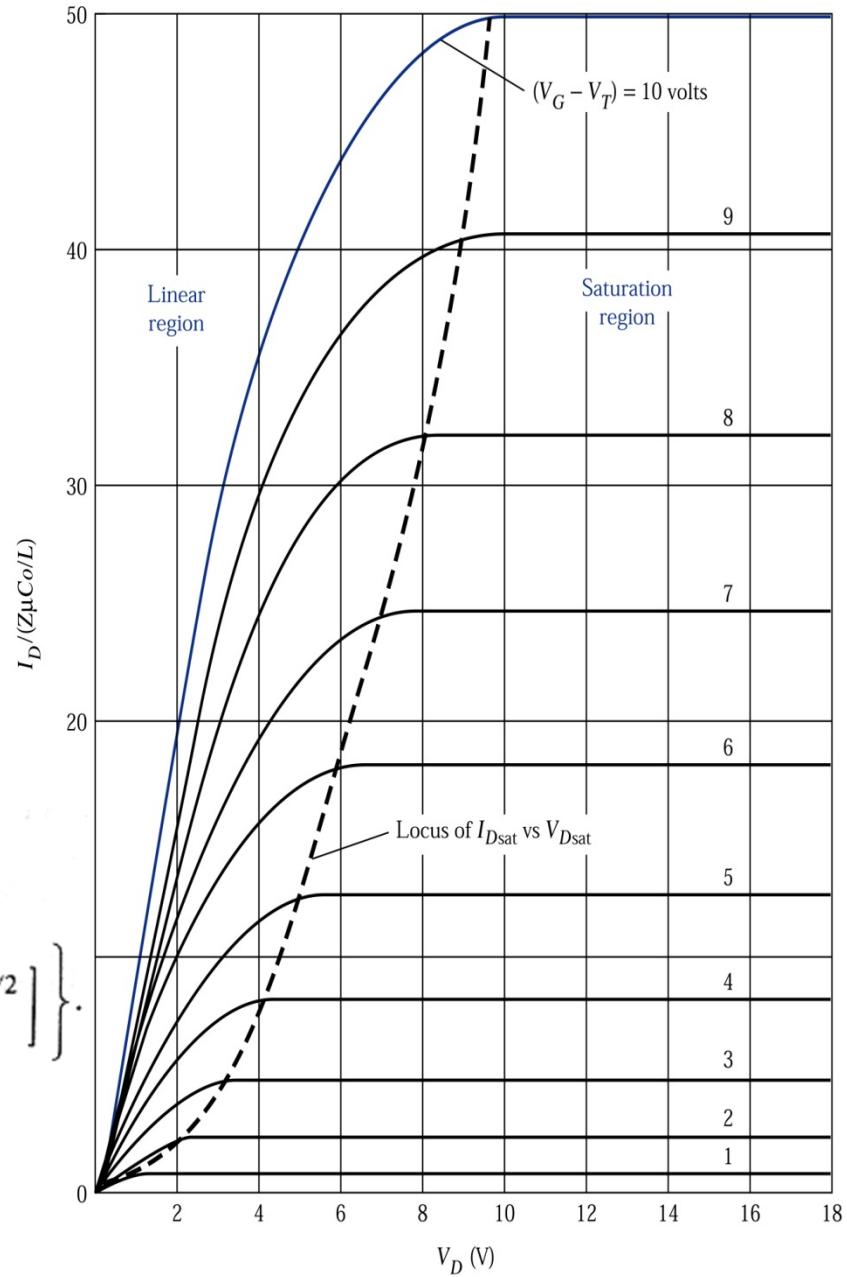
$$dR = \frac{dy}{gL} = \frac{dy}{Z\mu_n |Q_n(y)|} \quad (31)$$

$$dV = I_D \overset{\text{i不變}}{\uparrow} dR = \frac{I_D dy}{Z\mu_n |Q_n(y)|} \quad (32)$$

Figure 5.24.
Idealized drain characteristics of a MOSFET. For $V_D \geq V_{Dsat}$, the drain current remains constant.

I_D vs V_D 之 general eq.

$$I_D \approx \frac{Z}{L} \mu_n C_o \left\{ \left[V_G - 2\psi_B - \frac{V_D}{2} \right] V_D - \frac{2}{3} \frac{\sqrt{2\epsilon_s q N_A}}{C_o} \left[(V_D + 2\psi_B)^{3/2} - (2\psi_B)^{3/2} \right] \right\} \quad (33)$$



Linear:

V_D 很小時,(33)可化成:
$$I_D = \frac{Z}{L} \mu_n C_o [(V_G - V_T)V_D - \left(\frac{1}{2} + \frac{\sqrt{\epsilon_s q N_A / \Phi_B}}{4C_o}\right) V_D^2]$$

$$I_D \simeq \frac{Z}{L} \mu_n C_o (V_G - V_T) V_D \quad \text{for } V_D \ll (V_G - V_T) \quad (34)$$

:linear relation/線性區

$$V_T \simeq \frac{\sqrt{2\epsilon_s q N_A (2\psi_B)}}{C_o} + 2\psi_B. \quad (35)$$

*For small V_D (0.1,0.05), I_D vs V_G 曲線之切線即為 V_T 

$$g_D \equiv \left. \frac{\partial I_D}{\partial V_D} \right|_{V_G = \text{const}} \simeq \frac{Z}{L} \mu_n C_o (V_G - V_T) \quad (36)$$

$$g_m \equiv \left. \frac{\partial I_D}{\partial V_G} \right|_{V_D = \text{const}} \simeq \frac{Z}{L} \mu_n C_o V_D. \quad (37)$$

Sat.*pinch off $\equiv Q_n(L)=0$, 令(27)=0得

$$V_{Dsat} \simeq V_G - 2\psi_B + K^2 \left[1 - \sqrt{1 + 2V_G/K^2} \right] \quad (38)$$

*(38)代入(33)

$$I_{Dsat} \simeq \frac{Z \mu_n \epsilon_{ox}}{2dL} (V_G - V_T)^2. \quad (39)$$

$g_D=0$

$$g_m \equiv \left. \frac{\partial I_D}{\partial V_G} \right|_{V_D = \text{const}} = \frac{Z \mu_n \epsilon_{ox}}{dL} (V_G - V_T). \quad (40)$$

T_{ox}

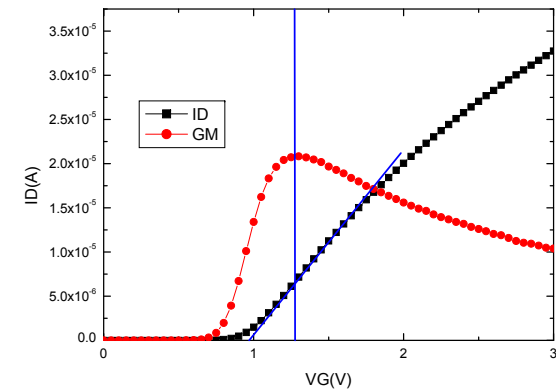


Figure 5.25. Subthreshold characteristics of a MOSFET.

*MOSFET 做為 switch 時, 特別重要

Subthreshold: surface at weak inversion
 I_D is dominated by diffusion current

$$I_D = -qAD_n \frac{dn}{dy} = qAD_n \frac{n(0) - n(L)}{L} \quad (41)$$

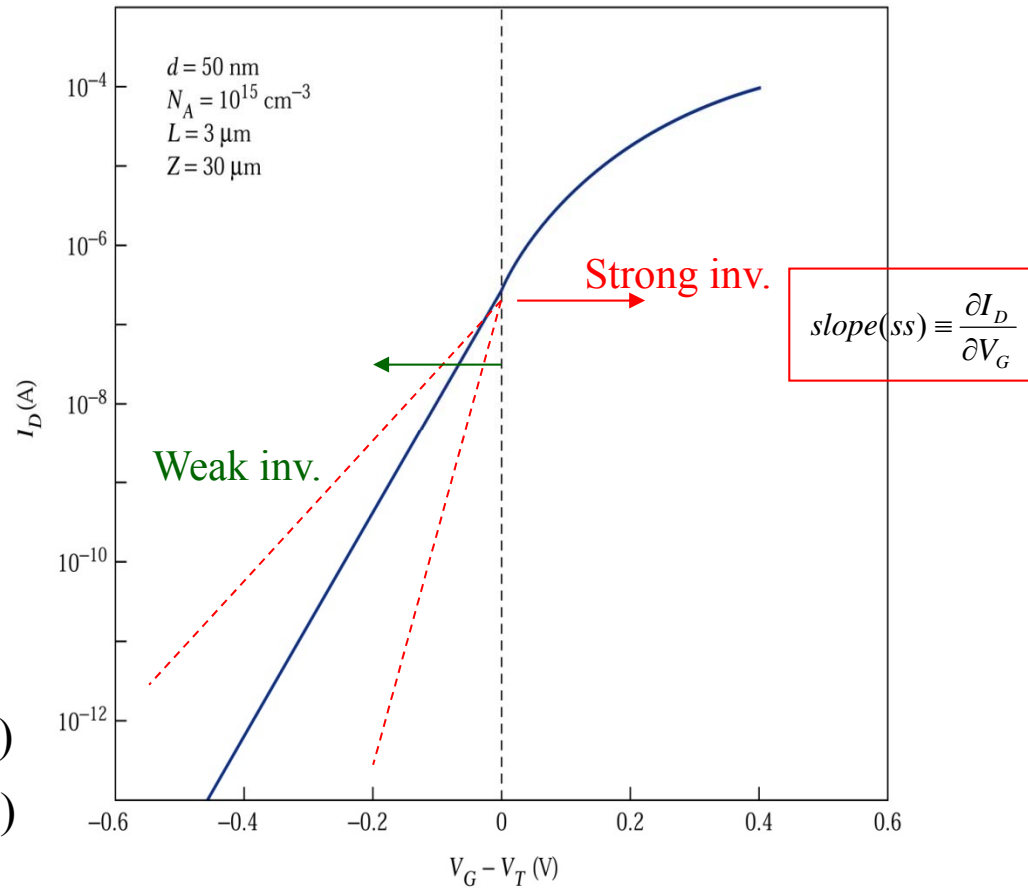
*因為尚未 strong inv., 電流以 diff. 為主

$$n(0) = n_i e^{q(\psi_s - \psi_B)/kT} \quad (42a)$$

$$n(L) = n_i e^{q(\psi_s - \psi_B - V_D)/kT} \quad (42b)$$

$$I_D = \frac{qAD_n n_i e^{-q\psi_B/kT}}{L} (1 - e^{-qV_D/kT}) e^{q\psi_s/kT} \quad (43)$$

$$I_D \sim e^{q(V_G - V_T)/kT} \quad (44)$$



$$\Psi_s \approx K(V_G - V_T)$$

Log I_D vs $(V_G - V_T)$ 為直線

$$\Psi_s \approx K(V_G - V_T)$$

請參考 p.446, SM Sze, Physics of Semiconductor Devices (大施敏)

where we have used the relation $D_n = \mu_n kT/q$, and a is given by Eq. 33. The surface potential ψ_s is related to the gate voltage as follows:^{18,19}

$$\psi_s = (V_G - V_{FB}) - \frac{a^2}{2\beta} \left\{ \left[1 + \frac{4}{a^2} (\beta V_G - \beta V_{FB} - 1) \right]^{1/2} - 1 \right\}. \quad (41)$$

$$a \equiv \sqrt{2}(\epsilon_s/L_D)/C_i = 2(\epsilon_s/\epsilon_i)(d/L_D). \quad (33) \quad \beta = \frac{KT}{q}$$

18 J. R. Brews, "A Charge-Sheet Model of the MOSFET," *Solid State Electron.*, **21**, 345 (1978).

19 J. R. Brews, "Subthreshold Behavior of Uniformly and Nonuniformly Doped Long-Channel MOSFET," *IEEE Trans. Electron Devices*, **ED-26**, 1282 (1979).

*enhancement mode為主

N

P

Type	Cross Section	Output Characteristics	Transfer Characteristics
<u>n-Channel Enhancement</u> (Normally Off)			
n-Channel Depletion (Normally On)			
<u>p-Channel Enhancement</u> (Normally Off)			
p-Channel Depletion (Normally On)			

Figure 5.26. Cross section, output, and transfer characteristics of four types of MOSFETs.

Threshold Voltage Control

$$\begin{aligned}
 V_T &\simeq V_{FB} + 2\psi_B + \frac{\sqrt{2\epsilon_s q N_A (2\psi_B)}}{C_o} \quad (Q_n \uparrow + Q_{sc}) \\
 &= \left[\phi_{ms} - \frac{Q_f}{C_o} \right] + 2\psi_B + \frac{\sqrt{4\epsilon_s q N_A \psi_B}}{C_o} \quad (45)
 \end{aligned}$$

故使用 ion-implant, 改變 Substrate doping, 而調 V_{T0}

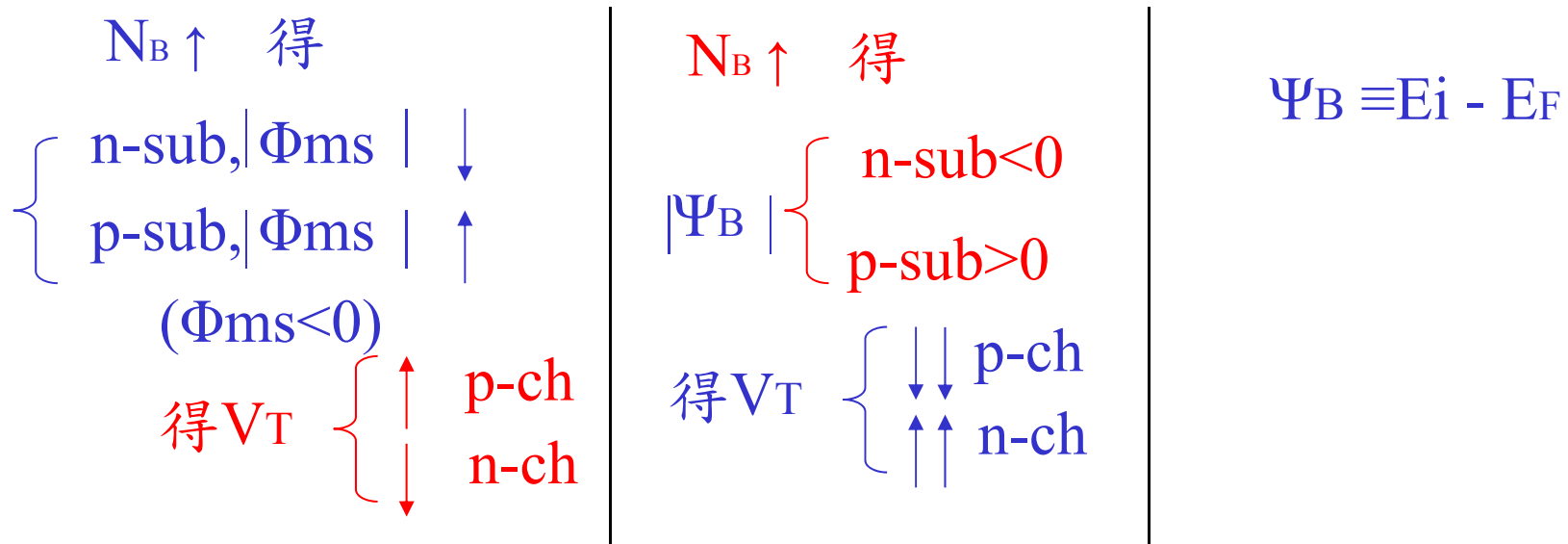
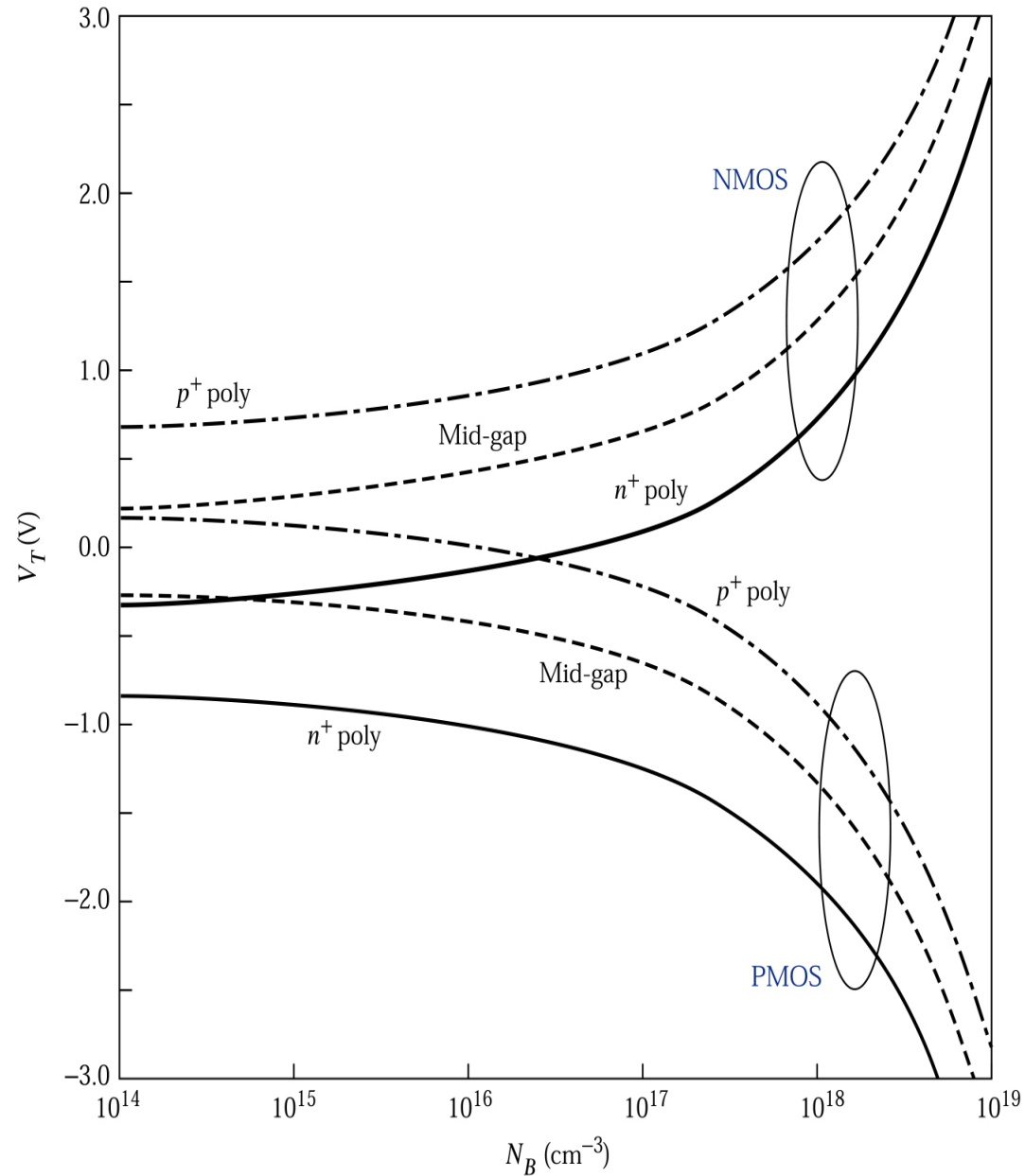


Figure 5.27.

Calculated threshold voltage of n -channel (V_{Tn}) and p -channel (V_{Tp}) MOSFETs as a function of impurity concentration, for devices with n^+ , p^+ polysilicon, and mid-gap work function gates assuming zero fixed charge. The thickness of the gate oxide is 5 nm. NMOS, n -channel MOSFET; PMOS, p -channel MOSFET.



EXAMPLE 6

For an n -channel n^+ -polysilicon-SiO₂-Si MOSFET with $N_A = 10^{17} \text{ cm}^{-3}$ and $Q_f/q = 5 \times 10^{11} \text{ cm}^{-2}$, calculate V_T for a gate oxide of 5 nm. What is the boron ion dose required to increase V_T to 0.6 V? Assume that the implanted acceptors form a sheet of negative charge at the Si-SiO₂ interface.

SOLUTION From the examples in Section 6.1, we have $C_o = 6.9 \times 10^{-7} \text{ F/cm}^2$, $2\psi_B = 0.84 \text{ V}$, $V_{FB} = -1.1 \text{ V}$. Therefore, from Eq. 45 (with $V_{BS} = 0$),

$$\begin{aligned} V_T &= V_{FB} + 2\psi_B + \frac{\sqrt{2\epsilon_s q N_A (2\psi_B)}}{C_o} \\ &= -1.1 + 0.84 + \frac{\sqrt{2 \times 11.9 \times 8.85 \times 10^{-14} \times 1.6 \times 10^{-19} \times 10^{17} \times 0.84}}{6.9 \times 10^{-7}} \\ &= -0.02 \text{ V.} \end{aligned}$$

The boron charge causes a flat-band shift of qF_B/C_o . Thus,

$$\begin{aligned} 0.6 &= -0.02 + \frac{qF_B}{6.9 \times 10^{-7}}, \\ F_B &= \frac{0.62 \times 6.9 \times 10^{-7}}{1.6 \times 10^{-19}} = 2.67 \times 10^{12} \text{ cm}^{-2}. \end{aligned}$$

EXAMPLE 7

For an n -channel field transistor with $N_A = 10^{17} \text{ cm}^{-3}$ and $Q_f/q = 5 \times 10^{11} \text{ cm}^{-2}$, calculate V_T for a gate oxide (i.e., the field oxide) of 500 nm.

SOLUTION $C_o = \epsilon_{ox} / d = 6.9 \times 10^{-9} \text{ F/cm}^2$.

From Exs. 2 and 3, we have $2\psi_B = 0.84 \text{ V}$, and $V_{FB} = -1.1 \text{ V}$.

Therefore, from Eq.45 (with $V_{BS} = 0$)

$$\begin{aligned} V_T &= V_{FB} + 2\psi_B + \frac{\sqrt{2\epsilon_s q N_A (2\psi_B)}}{C_o} \\ &= -1.1 + 0.84 + \frac{\sqrt{2 \times 11.9 \times 8.85 \times 10^{-14} \times 1.6 \times 10^{-19} \times 10^{17} \times 0.84}}{6.9 \times 10^{-9}} \\ &= 24.12 \text{ V.} \end{aligned}$$

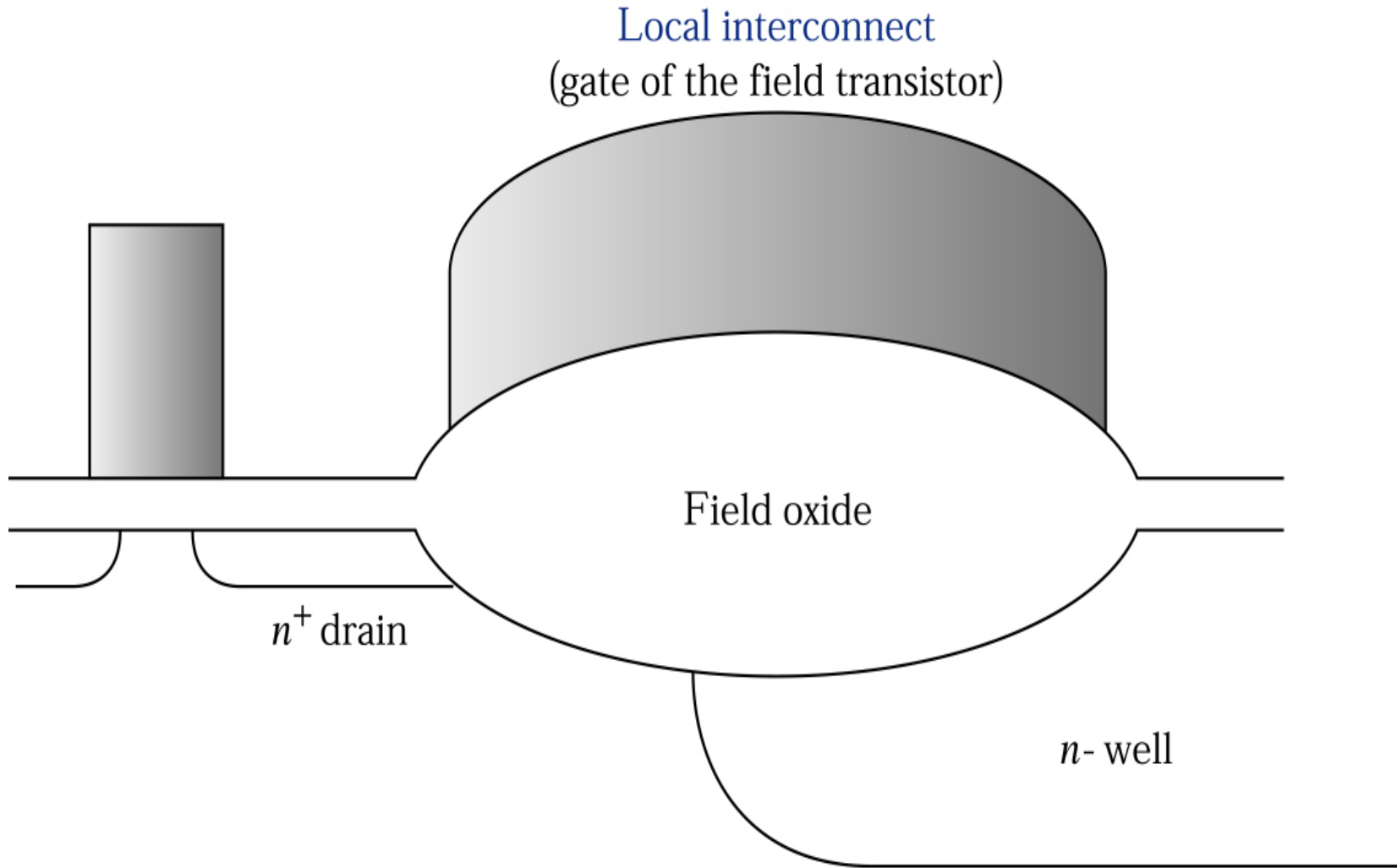


Figure 5.28. Cross section of a parasitic field transistor in an n -well structure.

若 Substrate 加反向偏壓 V_{BS}

$$Q'_B = -\sqrt{2q\epsilon_s N_A(2\psi_B + V_{BS})}$$

Space charge

$$\Delta V_T = \frac{\sqrt{2q\epsilon_s N_A}}{C_{ox}} (\sqrt{2\psi_B + V_{BS}} - \sqrt{2\psi_B}) \quad (46)$$

$\left\{ \begin{array}{l} V_{BS} < 0, V_T \text{ 增加.} \\ V_{BS} > 0, V_T \text{ 減少.} \end{array} \right.$

以 V_{BS} 調 V_T , 即 $|V_{BS}| \uparrow \rightarrow V_T \uparrow$

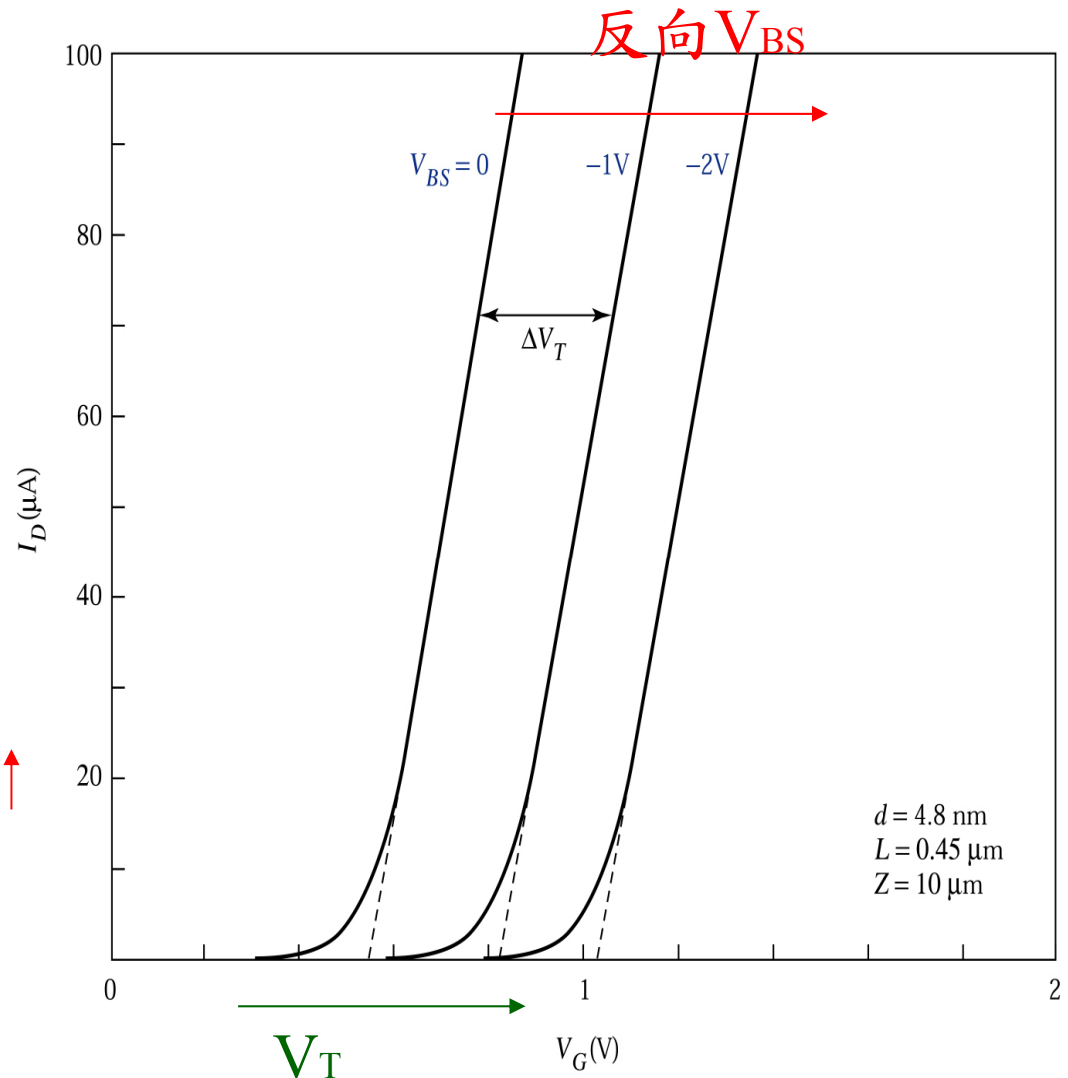
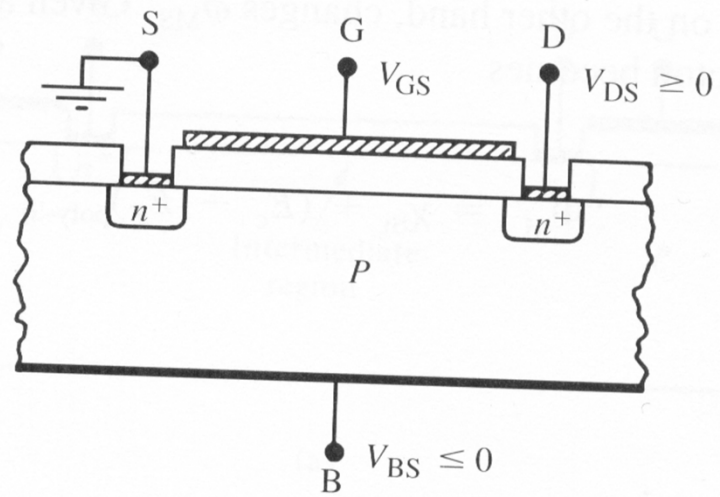
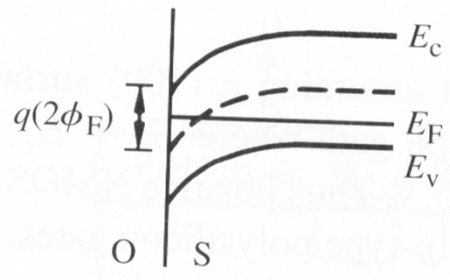


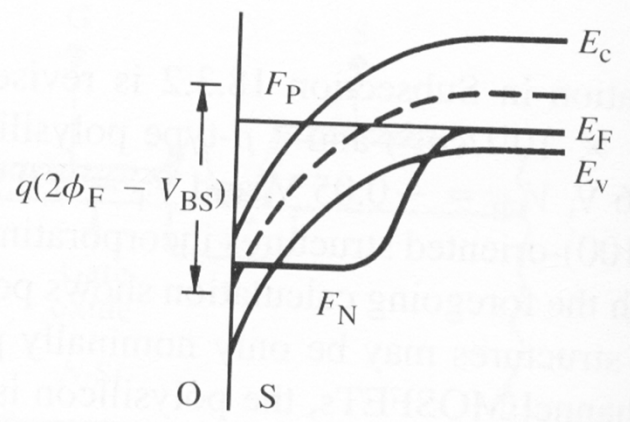
Figure 5.29. Threshold voltage adjustment using substrate bias.



(a)



(b)



(c)